TARDEC

(1)

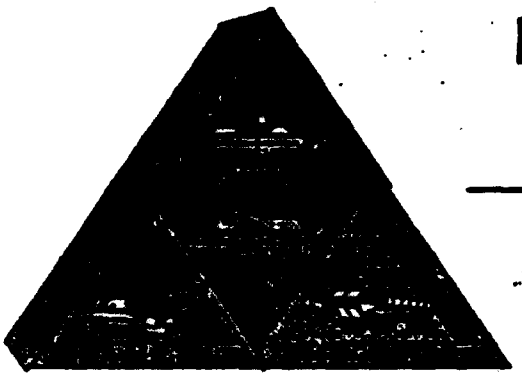

Technical Report

No. 13599

RESPONSE ANALYSIS FOR ATAS TURRET UNDER GUN SHOCK, THERMAL GRADIENT AND DYNAMIC VIBRATIONS USING FINITE ELEMENT ANALYSIS.

By SAMIR KHOURDAJI, M.Sc, P.E.
Engr Des Div

U.S. Army Tank-Automotive Command
Research, Development, and Engineering Center
Warren, Michigan 48397-5000

DISCLAIMER NOTICE

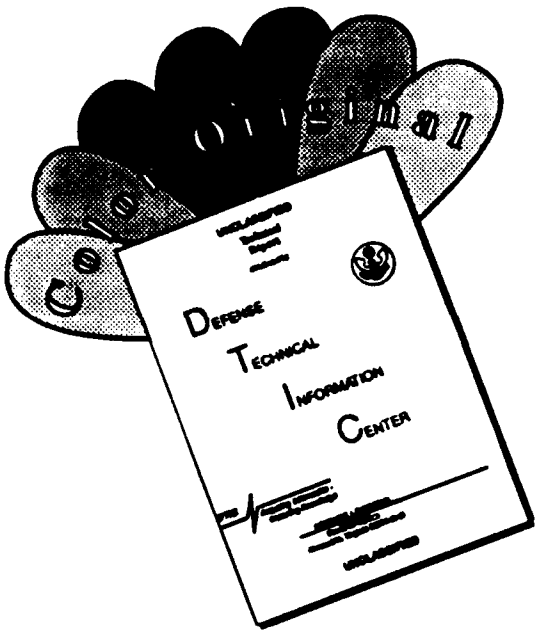

THIS DOCUMENT IS BEST QUALITY AVAILABLE. THE COPY FURNISHED TO DTIC CONTAINED A SIGNIFICANT NUMBER OF COLOR PAGES WHICH DO NOT REPRODUCE LEGIBLY ON BLACK AND WHITE MICROFICHE.

Unclassified
SECURITY CLASSIFICATION OF THIS PAGE

REPORT DOCUMENTATION PAGE

Form Approved
OMB No. 0704-0188
Exp. Date: Jun 30, 1986

1a. REPORT SECURITY CLASSIFICATION Unclassified	1b. RESTRICTIVE MARKINGS
2a. SECURITY CLASSIFICATION AUTHORITY	3. DISTRIBUTION/AVAILABILITY OF REPORT Approved for Public Release Distribution is Unlimited
2b. DECLASSIFICATION/DOWNGRADING SCHEDULE	
4. PERFORMING ORGANIZATION REPORT NUMBER(S)	5. MONITORING ORGANIZATION REPORT NUMBER(S)
6a. NAME OF PERFORMING ORGANIZATION U.S. Army Tank-Automotive Command 6b. OFFICE SYMBOL (If applicable) AMSTA-TD	7a. NAME OF MONITORING ORGANIZATION
6c. ADDRESS (City, State, and ZIP Code) Warren, MI 48397-5000	7b. ADDRESS (City, State, and ZIP Code)
8a. NAME OF FUNDING/SPONSORING ORGANIZATION 8b. OFFICE SYMBOL (If applicable)	9. PROCUREMENT INSTRUMENT IDENTIFICATION NUMBER
8c. ADDRESS (City, State, and ZIP Code)	10. SOURCE OF FUNDING NUMBERS PROGRAM ELEMENT NO. / PROJECT NO. / TASK NO. / WORK UNIT ACCESSION NO.

11. TITLE (Include Security Classification)
Finite Element Stress Analysis for Advanced Technology Demonstrator (ATD2).
See Cover

12. PERSONAL AUTHOR(S)
Khourdaji, Samir

13a. TYPE OF REPORT	13b. TIME COVERED	14. DATE OF REPORT (Year, Month, Day)	15. PAGE COUNT
FINAL	FROM	93/11/26	53

16. SUPPLEMENTARY NOTATION

17. COSATI CODES			18. SUBJECT TERMS (Continue on reverse if necessary and identify by block number)
FIELD	GROUP	SUB-GROUP	Finite Element Turret, Gun Shock, Thermal, Vibration, Dynamic, Response

19. ABSTRACT (Continue on reverse if necessary and identify by block number)

The Finite Element Analysis is used to establish the response of ATD Turret to Gun Shock, Thermal Gradient and Terrain Vibrations.

20. DISTRIBUTION/AVAILABILITY OF ABSTRACT ☒ UNCLASSIFIED/UNLIMITED ☐ SAME AS RPT. ☐ DTIC USERS	21. ABSTRACT SECURITY CLASSIFICATION Unclassified
22a. NAME OF RESPONSIBLE INDIVIDUAL Samir Khourdaji	22b. TELEPHONE (Include Area Code) (313) 574-5875 22c. OFFICE SYMBOL AMSTA-TD

DD FORM 1473, 84 MAR 83 APR edition may be used until exhausted. All other editions are obsolete.

SECURITY CLASSIFICATION OF THIS PAGE
Unclassified

TABLE OF CONTENTS

LIST OF ILLUSTRATIONS

1. OBJECTIVE:

The purpose of this study is to evaluate the response of the Advanced Tank Armor System (ATAS) turret under the effects of gun shock, thermal gradient and terrain interaction. This response is expressed in terms of stress, deformation or induced vibrations. Knowledge of this response will determine if it impedes the performance of the two sensors mounted on top of the Turret. The Second-Generation Thermal Sight (SGTS) sensor is mounted on the right side casing, which is narrow and deep, and the Combat Protection System (CPS) sensor is mounted on the left casing, which is wider and shallower. This knowledge will also help devise the best strategy on how to adequately reduce the undesirable effects of certain responses.

In this study, the Finite Element Analysis (FEM) is utilized due to the complexity of the required calculations, also to achieve realistic accuracy of the final results, which is itself in the range of 0.01 in. The FEM method proved to be very efficient because only one model is needed for the various required analyses.

2. TURRET FEM MODEL:

The ATAS Turret Solid Model is constructed using an Intergraph CAD System (fig. 1), A 3-D surface model (fig. 2) is derived from this solid model. The latter is used to construct the Finite Element Model (fig. 3). This model consists of 1250 high-order (8-nodded) shell elements. The density (the maximum side length of any one element) is two inches. The choice of using higher order elements and dense finite element mesh is made to accurately capture all the details of the ATAS Turret, and to obtain the desired results with sufficient accuracy.

3. RESPONSE ANALYSIS:

The ATAS Turret FEM Model is constrained in the X,Y, and Z directions at the interface of the Turret ring with the hull casting. The external load in terms of gun shock, thermal gradient or dynamic vibrations is imposed on the FEM Model. The response of the FEM Model under these loading conditions is evaluated by conducting the appropriate analysis. The results are presented in the form of stress or displacement plots or vibration profiles.

4. GUN SHOCK RESPONSE:

The gun shock force is time-dependant as shown in fig. 4-1. Since no change in inertia occurs during firing and since the load magnitude and the material properties do not cause any non linearity in the model, the gun shock can be considered static force. The peak value of this force is 370,000 pounds, which is distributed equally on the two trunnions. The Finite Element Analysis is performed, and the results in terms of stresses and deformations in the Turret are shown in fig. 4-2 to 4-5.

5. THERMAL GRADIENT RESPONSE:

The temperature difference between the inside and the outside of the turret results in a thermal gradient that causes uneven expansion, which in turn causes thermal stresses to occur in the various plates of the ATAS turret. In this analysis a transient condition is assumed and two cases of thermal gradient are considered:

5.1 70/160 gradient : This occurs when the interior temperature is 70 degrees and the external temperature is 160. The resulting stresses and deformations are shown in fig. 5-1 to 5-5.

5.2 140/70 gradient : This occurs when the interior temperature is 140 degrees and the exterior temperature is 70 degrees. The displacements , which are shown in fig. 5-6 to 5-8, are opposite to those of the 70/160 gradient.

6. VIBRATIONS RESPONSE:

To establish the dynamic response of the ATAS turret, certain desired level of vibrations are induced and the Turret response is investigated. In this case, the road-test results of the Perryman paved course will be utilized to induce the necessary vibrations. In lieu of conducting comprehensive analysis on the FEM Model for the entire vehicle (which would be a complex and lengthy process, because the suspension also must be modeled), only the FEM Model for the ATAS Turret is utilized in conjunction with road-test results of Perryman paved course. These results are usually available in a form of Power Spectral Density (PSD) at various locations in the vehicle. Since the primary interest is the turret response, the PSD acceleration data for the turret ring obtained

for the Perryman course are shown in fig. 19 & 20. These data are averaged and combined with the PSD for the lower frequency of H bump course (fig. 6-21). The resulting PSD (fig. 6-1) is applied on the turret FEM model as base motion. Finally, the dynamic response analysis is conducted and the results are presented in the form of PSD and root mean square (RMS) displacement VS. frequency plots for various points of interest. The dynamic analysis consists of two parts; the modal analysis and the response analysis.

6.1 MODAL ANALYSIS: In this stage all modes which might affect the turret response are extracted. fig. 6-2 shows these modes and their natural frequencies. The deformed shape for mode 13, which has a frequency of 116 Hertz, are shown in figures 6-24 to 6-27.

6.2 DYNAMIC RESPONSE :

After the Modal Analysis is completed, the response analysis can be conducted. The PSD base acceleration data is applied on the turret FEM Model, and the turret response at various points are investigated. Initially, only 10 modes were used in the response analysis. but by examining the PSD displacements data for either of the two sensors (fig. 6-3 & 6-9), it becomes clear that displacements did not peak in the frequency range of the 10 modes considered. When the number of modes are increased to 19, the displacement has two high peaks. one corresponds to mode 13 which has a frequency of 116, and a smaller peak at mode 15 which has a frequency of 141. However, the printed results show that mode 19 calculation did not converge. Therefore, it must be excluded from the response analysis, because the program does not do this automatically. The analysis is performed once again without mode no. 19. The results are presented in the form of PSD or RMS for displacement or acceleration for the following points of interest.

Left Sensor	(fig. 6-3 to 6-8 & 6-22)
Right Sensor	(fig. 6-9 to 6-14 & 6-23)
Left Trunnion	(fig. 6-15 & 6-16)
Right trunnion	(fig. 6-17 & 6-18)

For both sensors the results are given at four points at the center of the flange. These points correspond to front, right, rear and left. Also, the results are given at center of the cover plates to approximate the average the values at these four points.

7. CONCLUSION:

The results of the response analysis of ATAS turret show that the maximum deflection in the vicinity of the CPS and SGTS sensors under gun shock, or under one of two thermal gradients considered (70/160 & 140/70), is less than .05 in. The dynamic deflections due to terrain interaction are much smaller (in the range of .001 in.). However, the frequencies at which these deflections occur are important to note, especially if they are close to the natural frequencies of the CPS or SGTS sensor, for they might induce undesirable vibrations. If the deflection under gun shock or thermal gradient is found to be excessive, then some structural modification to the Turret might be needed to insure that these deflections or undesirable vibrations are reduced to an acceptable level. In this case, these modifications must be validated through further analysis. In this analysis the PSD used for the base motion is 0.2 (G /Hz). however, the results are true for any PSD, provided that the final results are adjusted proportionally, except that the adjustment of RMS of the displacement or the acceleration is proportional to the square root of the ratio of the base motion PSD.

In this study, three types of analyses were conducted independently: gun shock, thermal gradient and dynamic vibrations. To represent more realistic field conditions, combining some of them might be necessary, for instance the turret can be first statically loaded by adding the weight of the gun, the armor and the auto-loader. Then the thermal gradient is applied and the thermal expansion is allowed to occur, after this the dynamic vibrations can be introduced. In this fashion the effects of the various process on each other and on the final results can be understood. In this study, it was not possible to accomplish that because of the large disc space required to save the restart files. This is primarily due to the large ATAS FEM model. However, this approach is recommended and will be followed in future similar analyses.

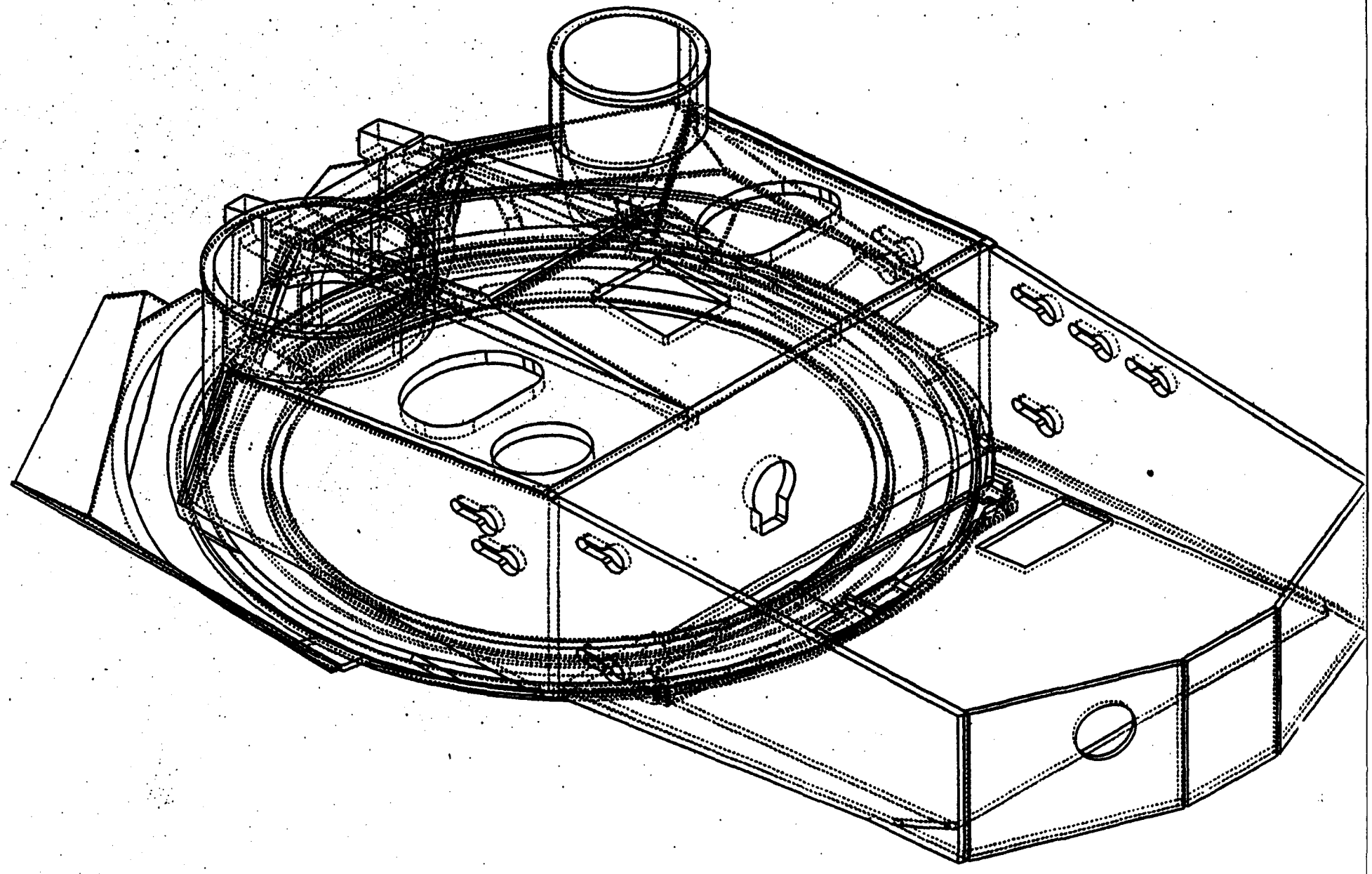

FIG 1. ATAS TURRET SOLID MODEL

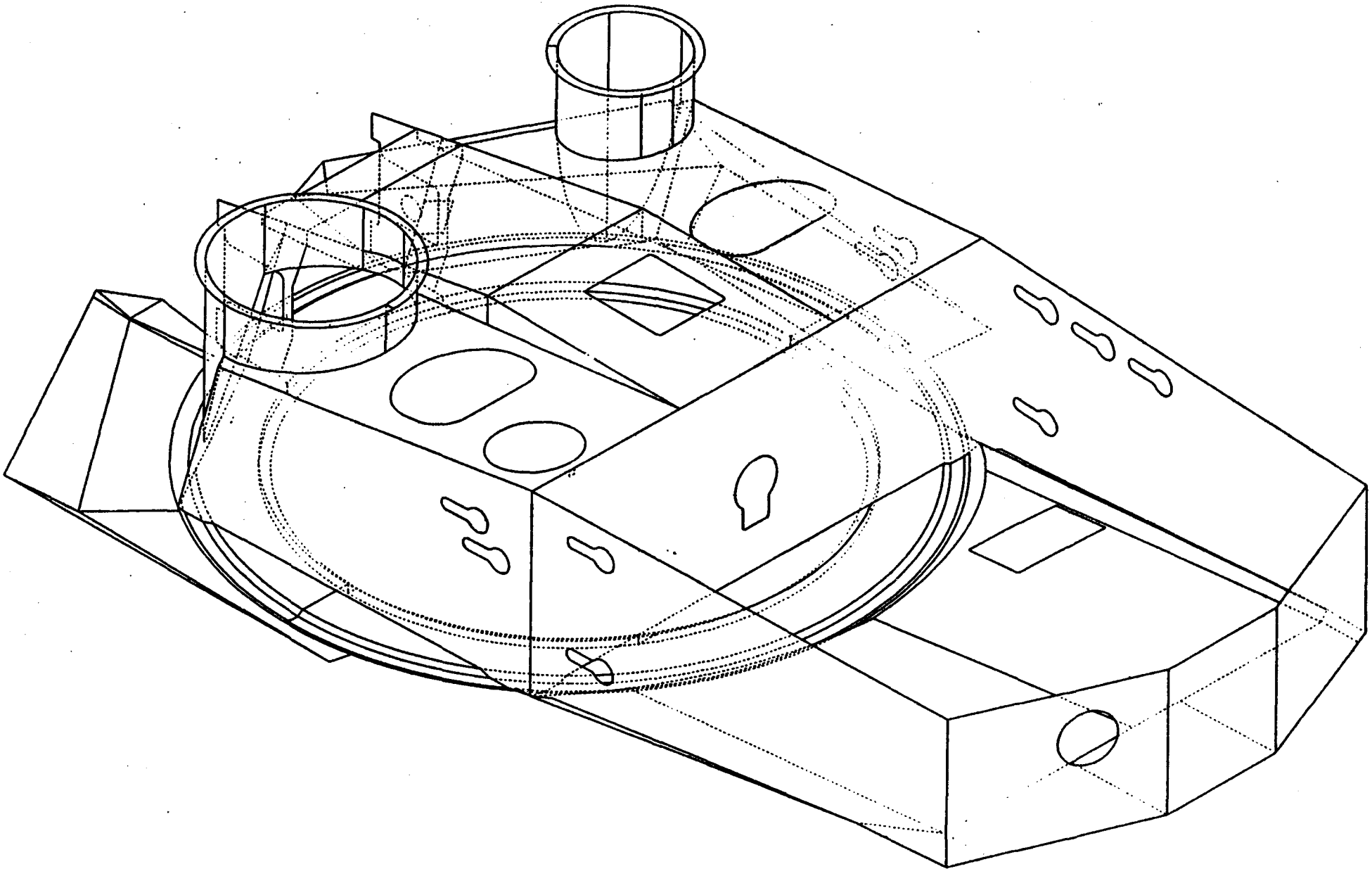

FIG. 2 ATAS TURRET 3D SURFACE MODEL

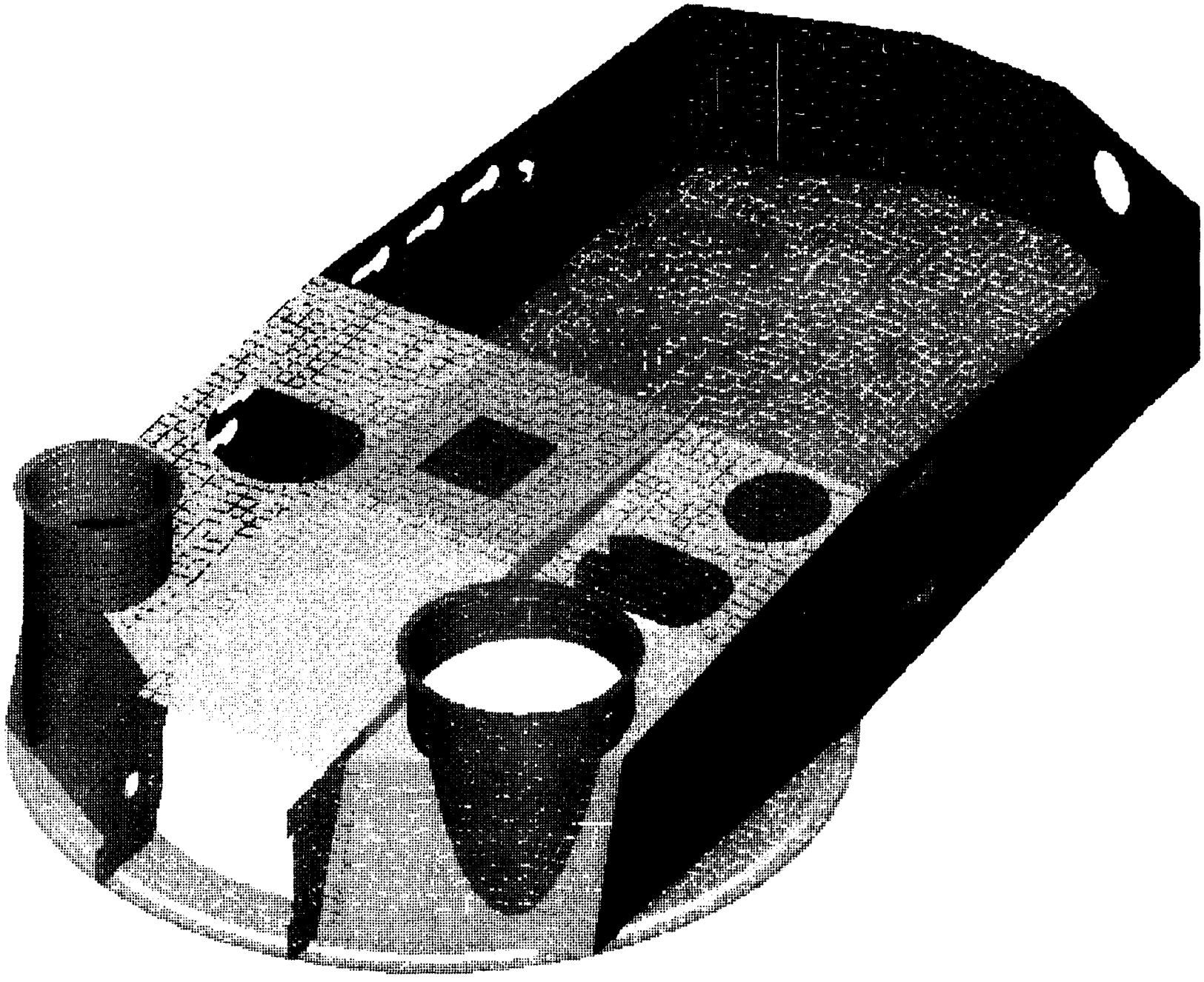

FIG 3. ATAS TURRET FEM MODEL

TANK TURRET BRANCH BENET LABS 3-93

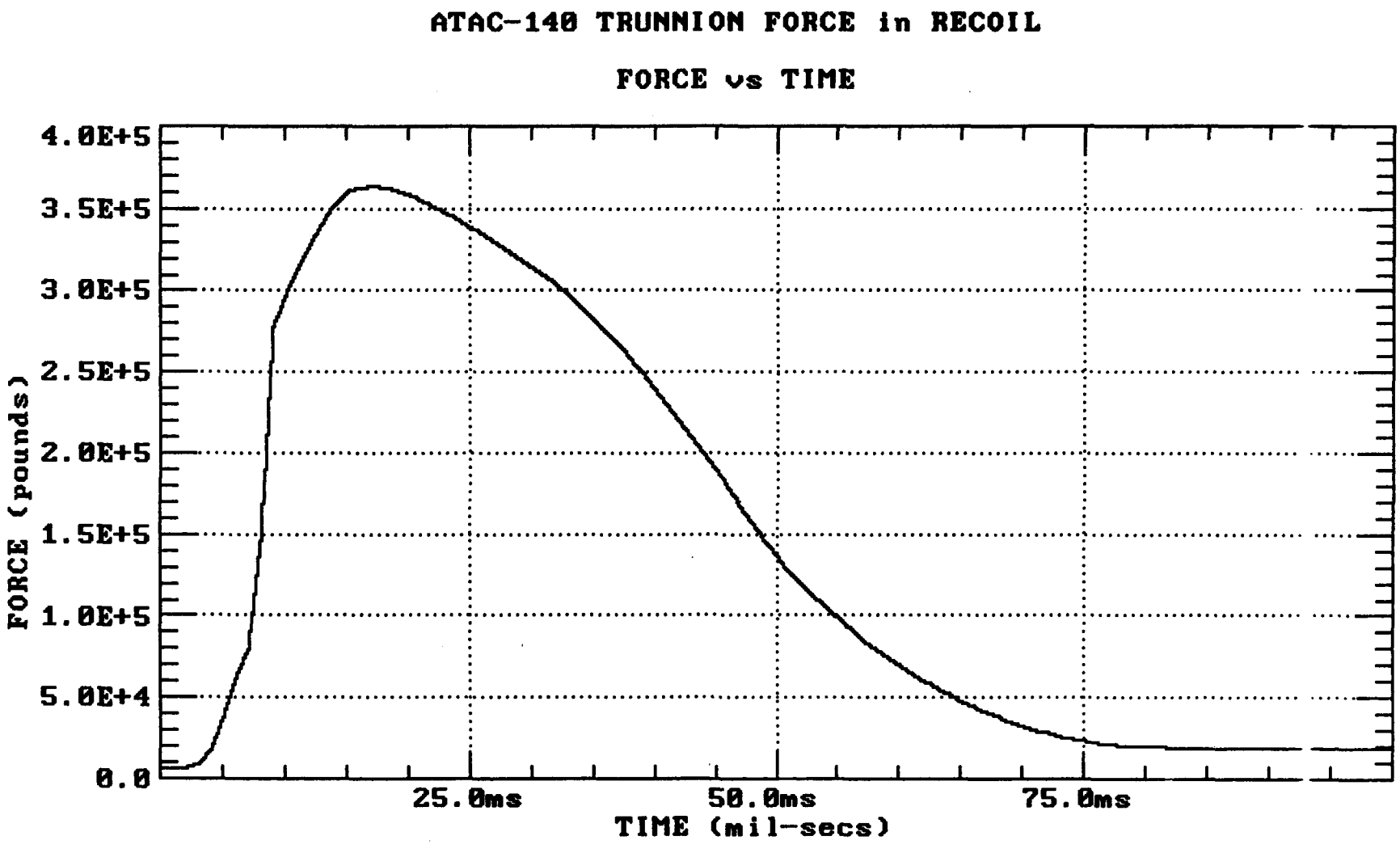

FIG 4-1 GUN FIRING IMPULSE

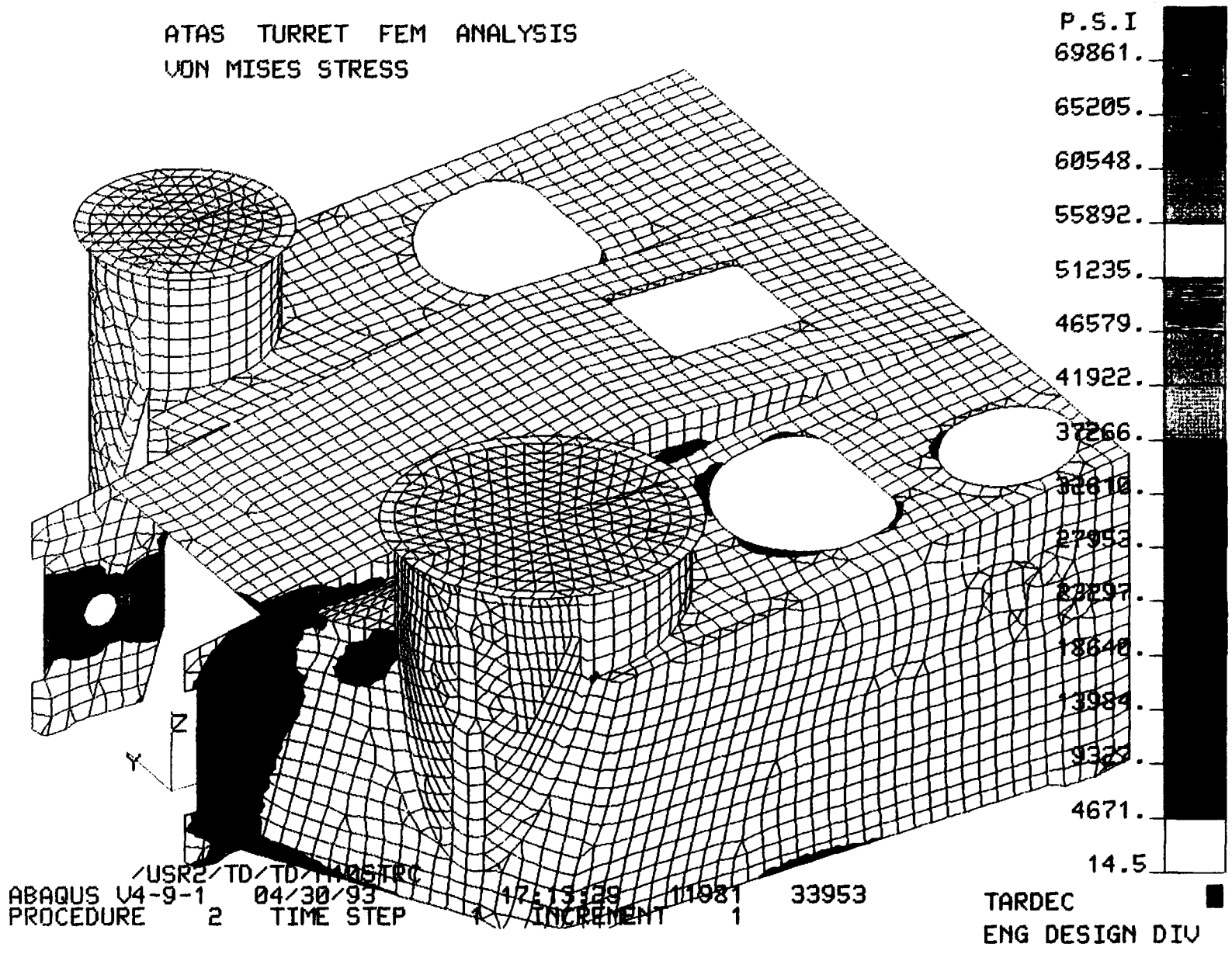

FIG.4-2 VON MISES STRESS UNDER GUN SHOCK

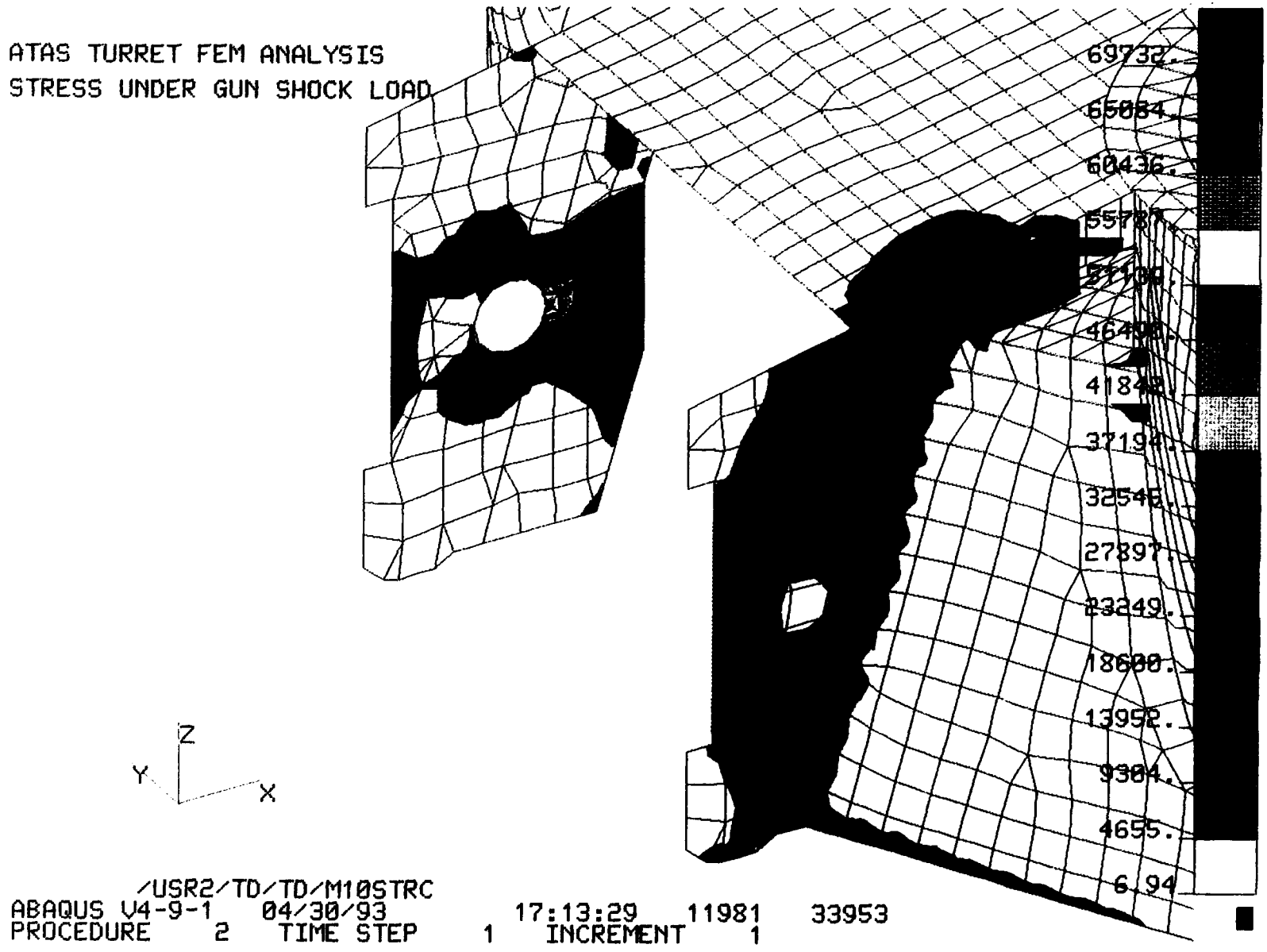

FIG. 4-3 VON MISES STRESS UNDER GUN SHOCK

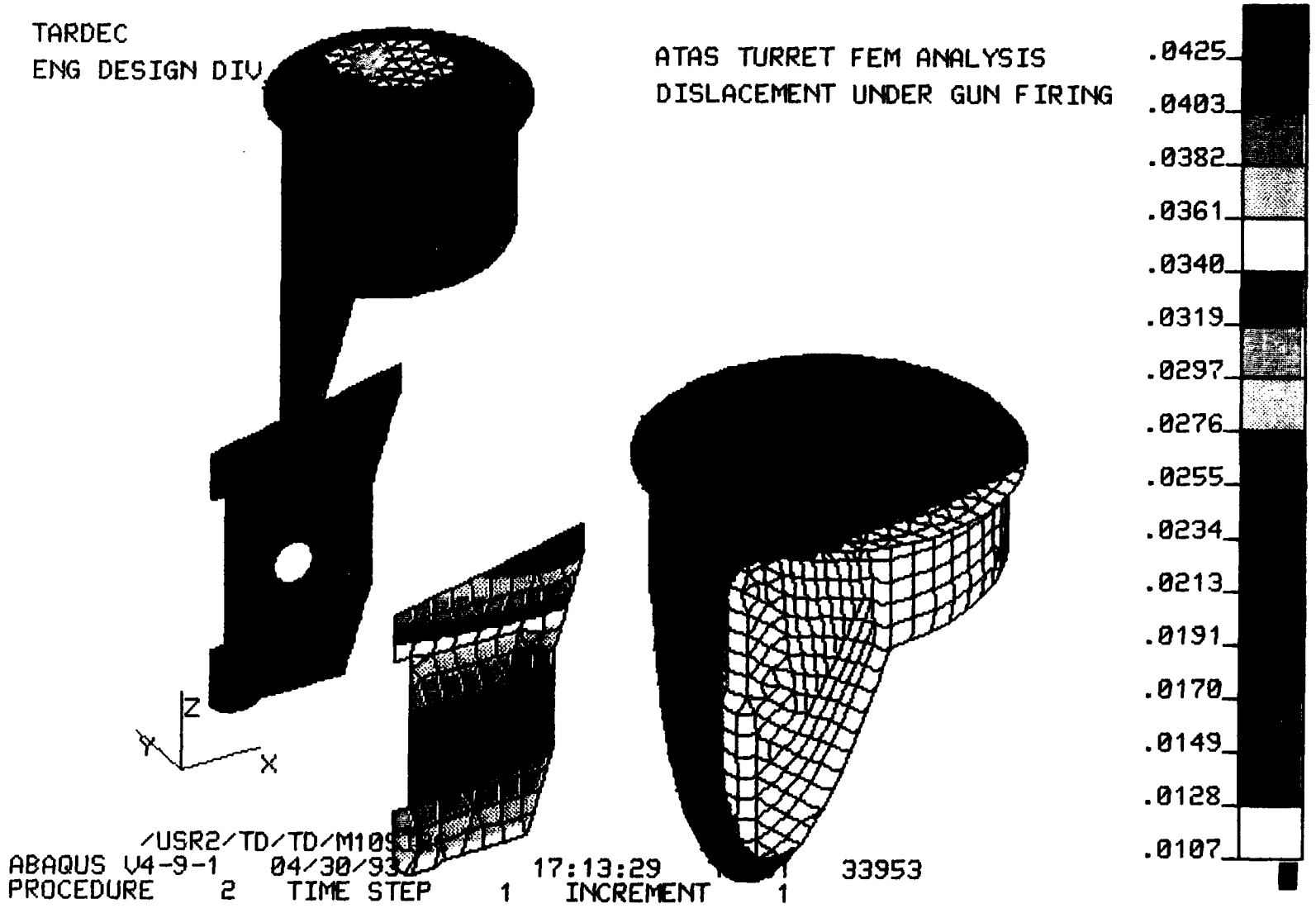

FIG. 4-4 TOTAL DISPLACEMENT UNDER GUN SHOCK

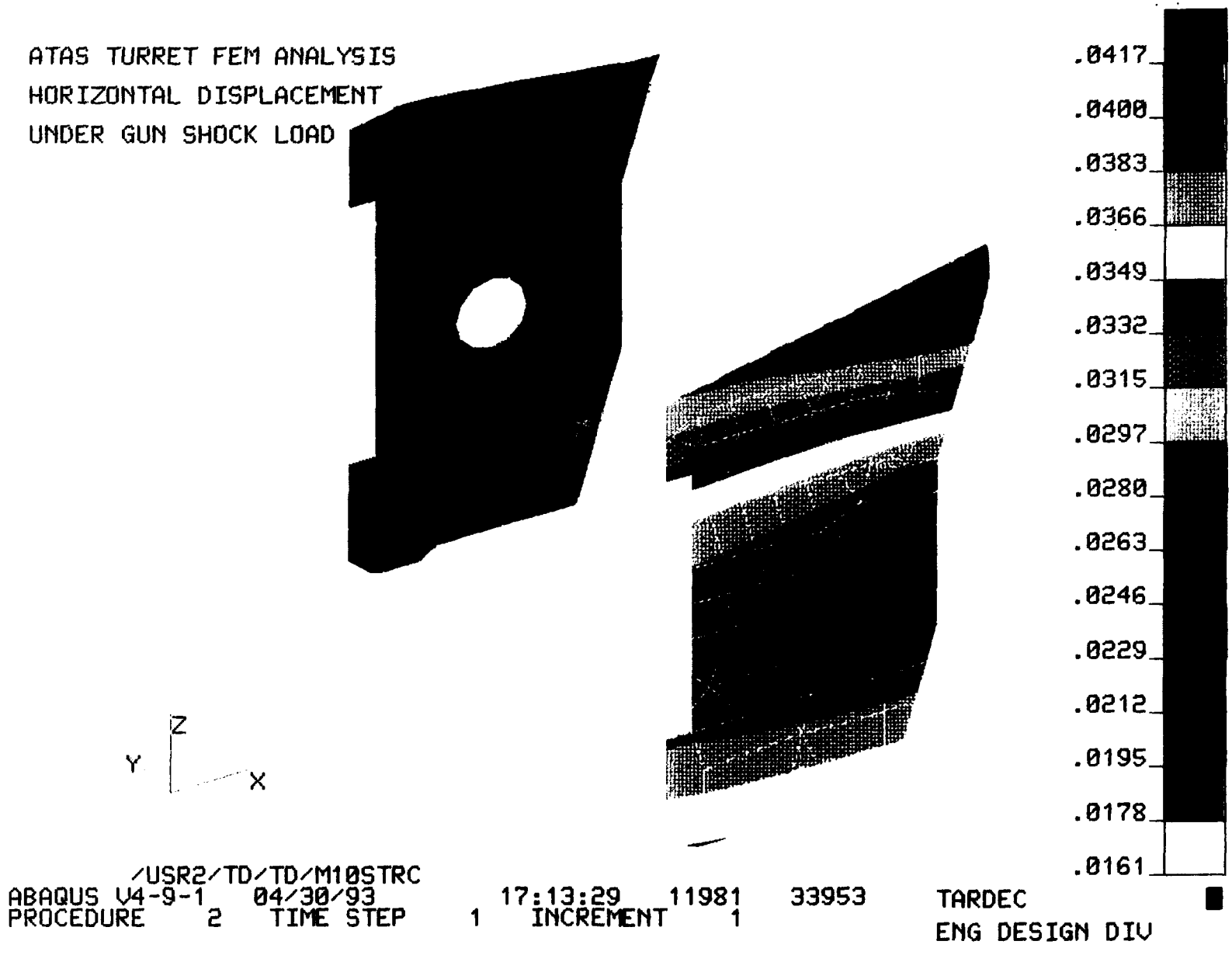

FIG.4-5 TOTAL DISPLACEMENT UNDER GUN SHOCK

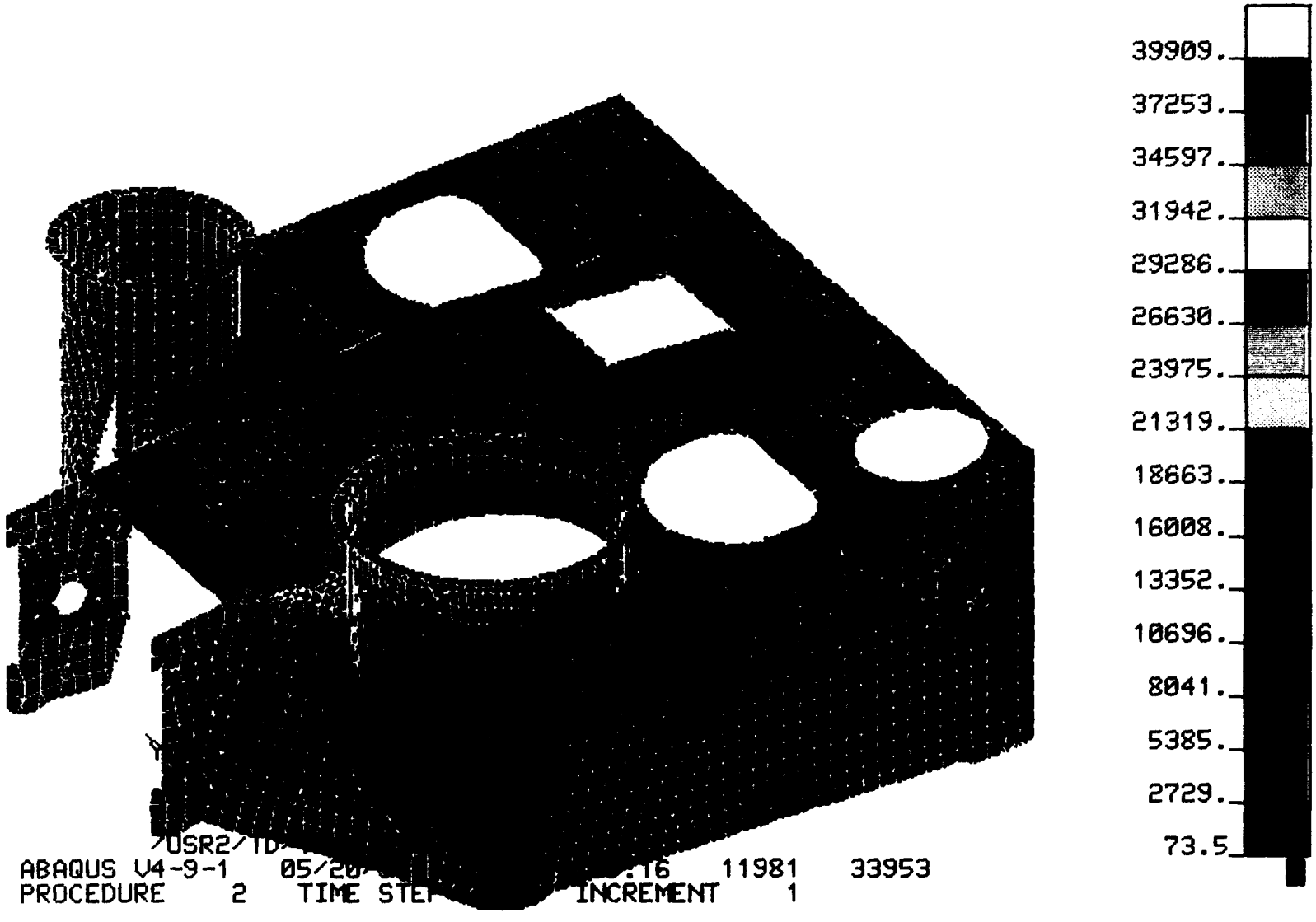

FIG. 5-1 VON MISES STRESS DUE TO (70/160) THERMAL GRADIENT

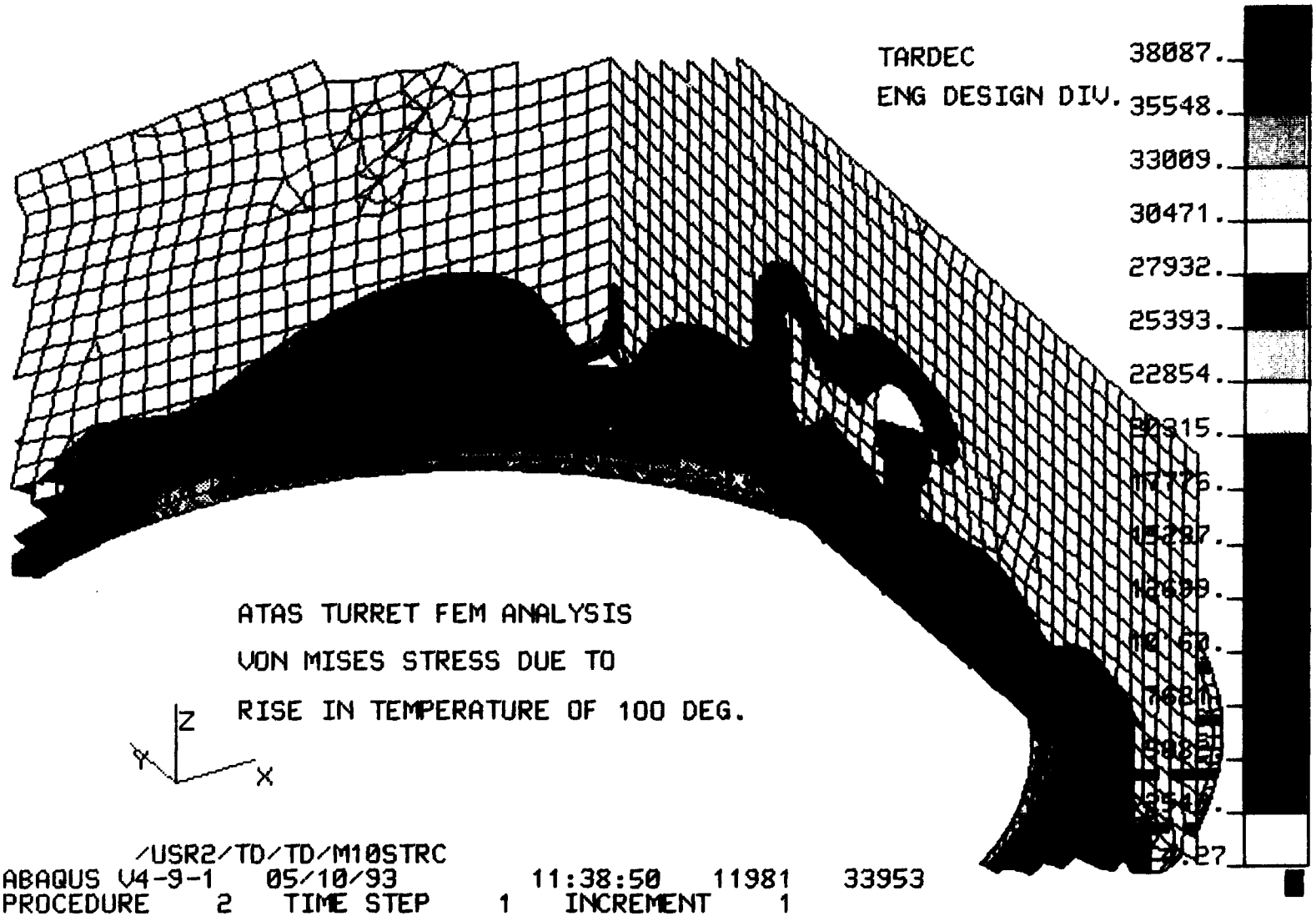

FIG.5-2 VON MISES STRESS DUE TO (70/160) THERMAL GRADIENT

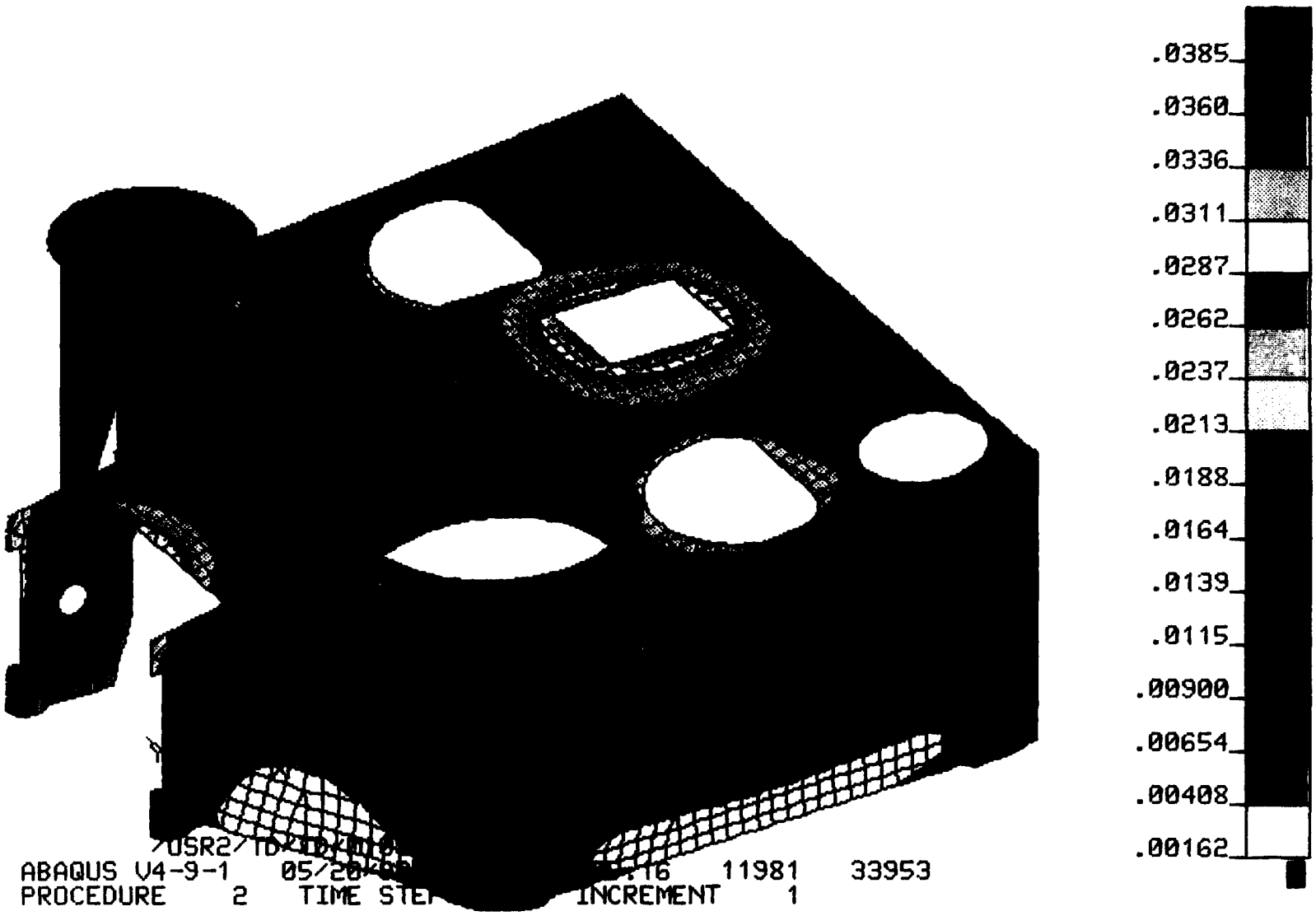

(TOTAL)

FIG 5-3. DISPLACEMENT IN ATAS TURRET DUE TO (70/160) THERMAL GRADIENTS

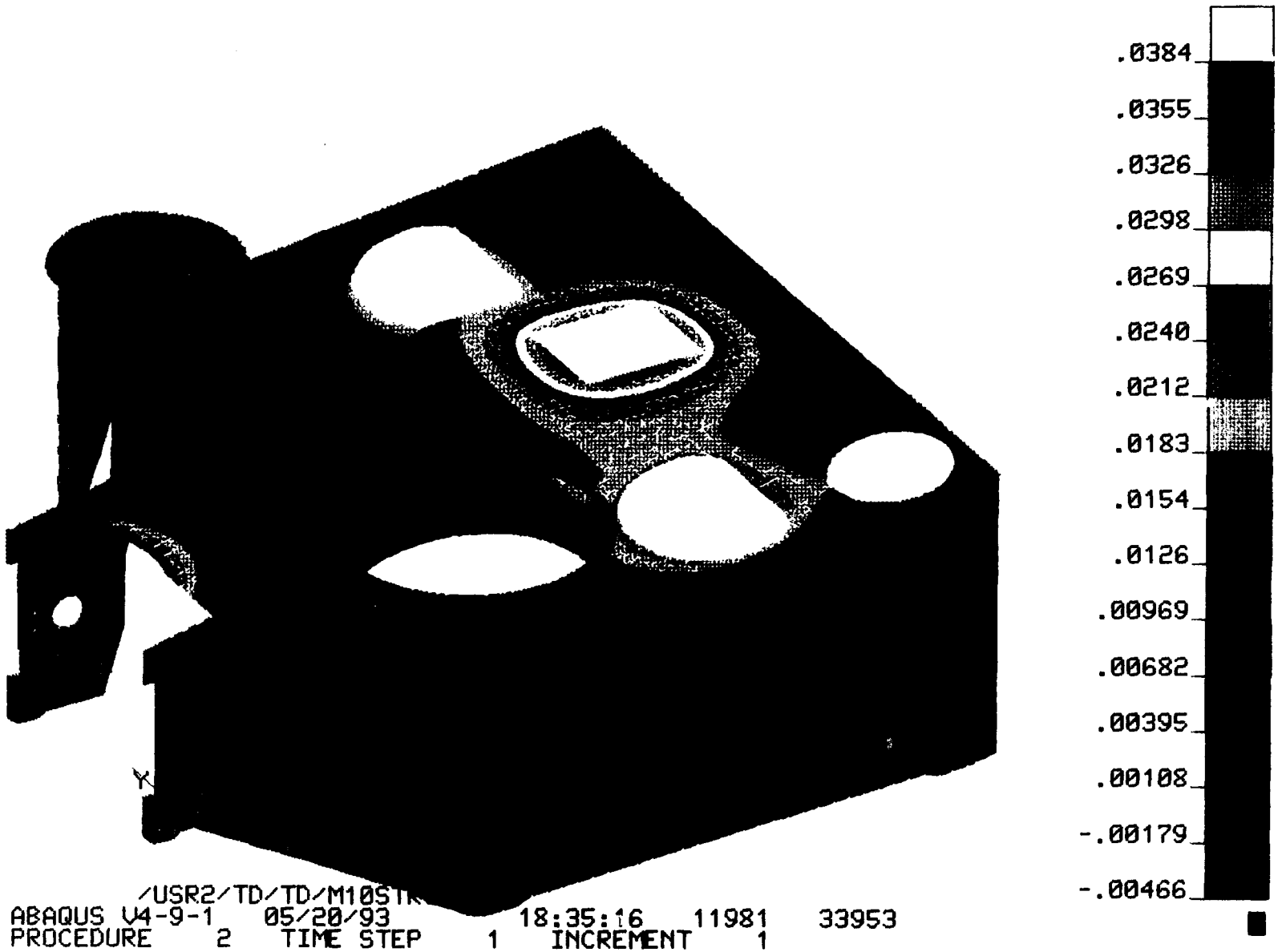

FIG.5-4 VERTICAL DISPLACEMENTS IN ATAS TURRET DUE TO (70/160) THERMAL GRADIENT

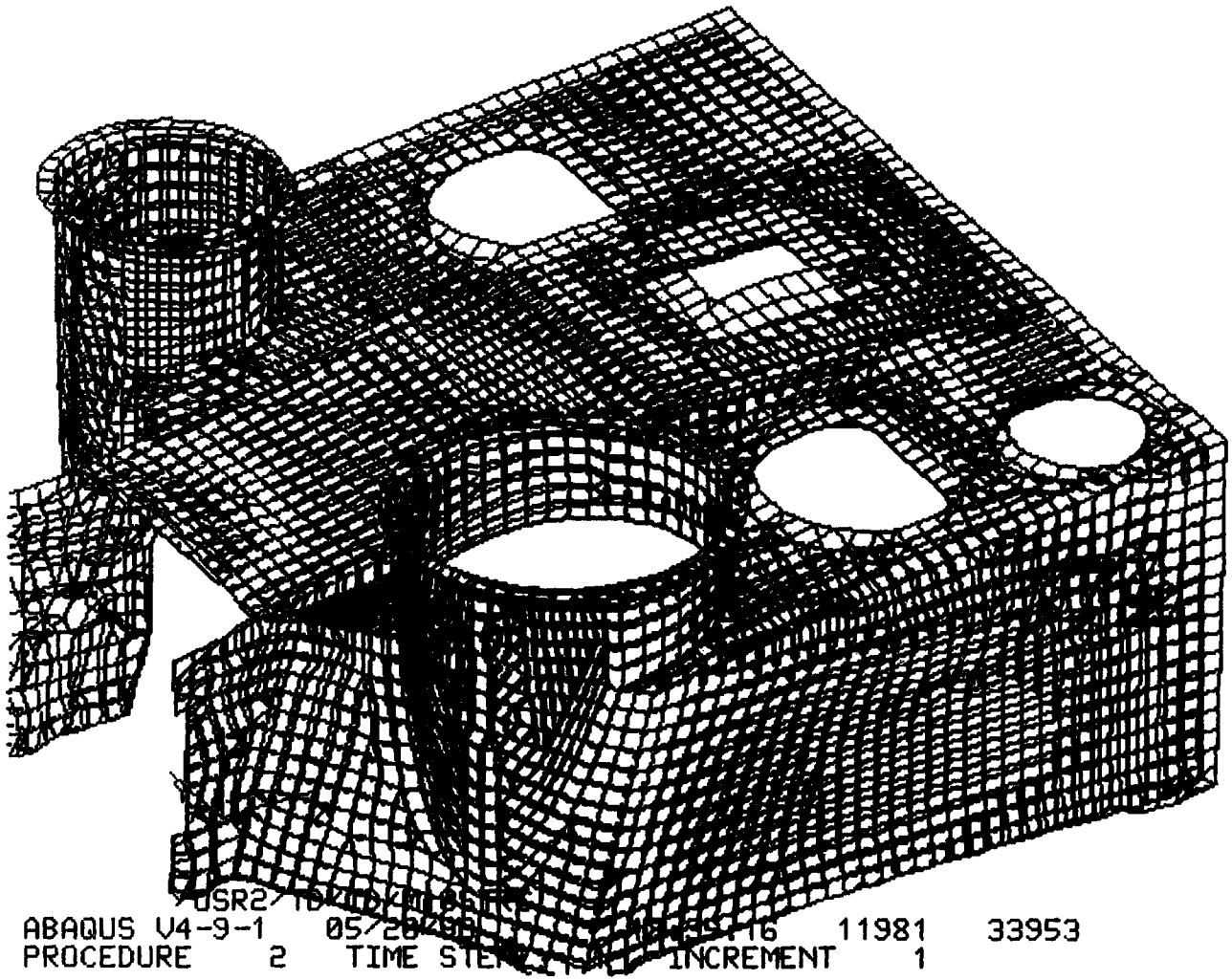

FIG. 5-5 ATAS TURRET DEFORMED SHAPE DUE TO THERMAL GRADIENT

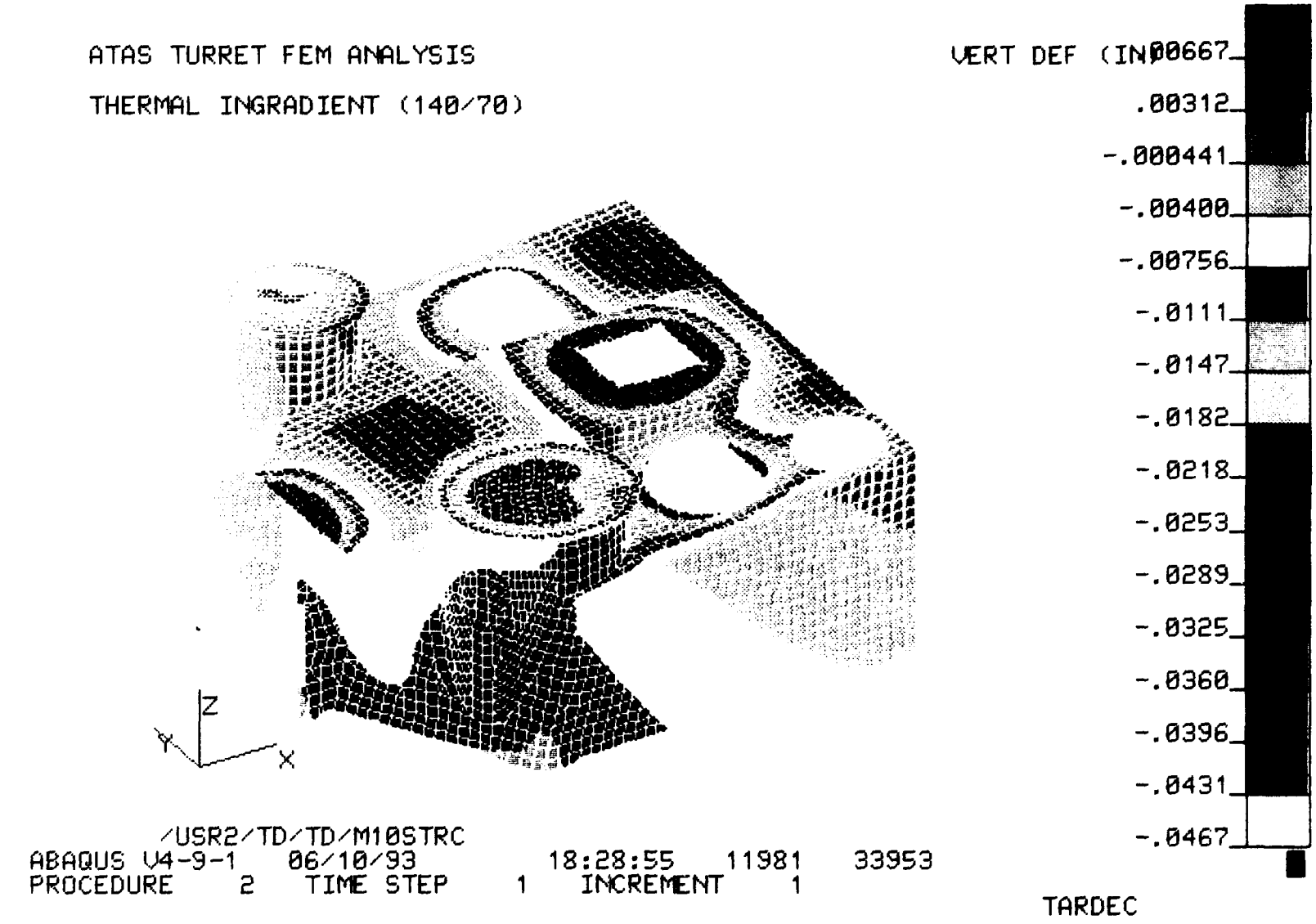

FIG5-6 VERTICAL DISPLACEMENT UNDER (140/70) GRADIENT

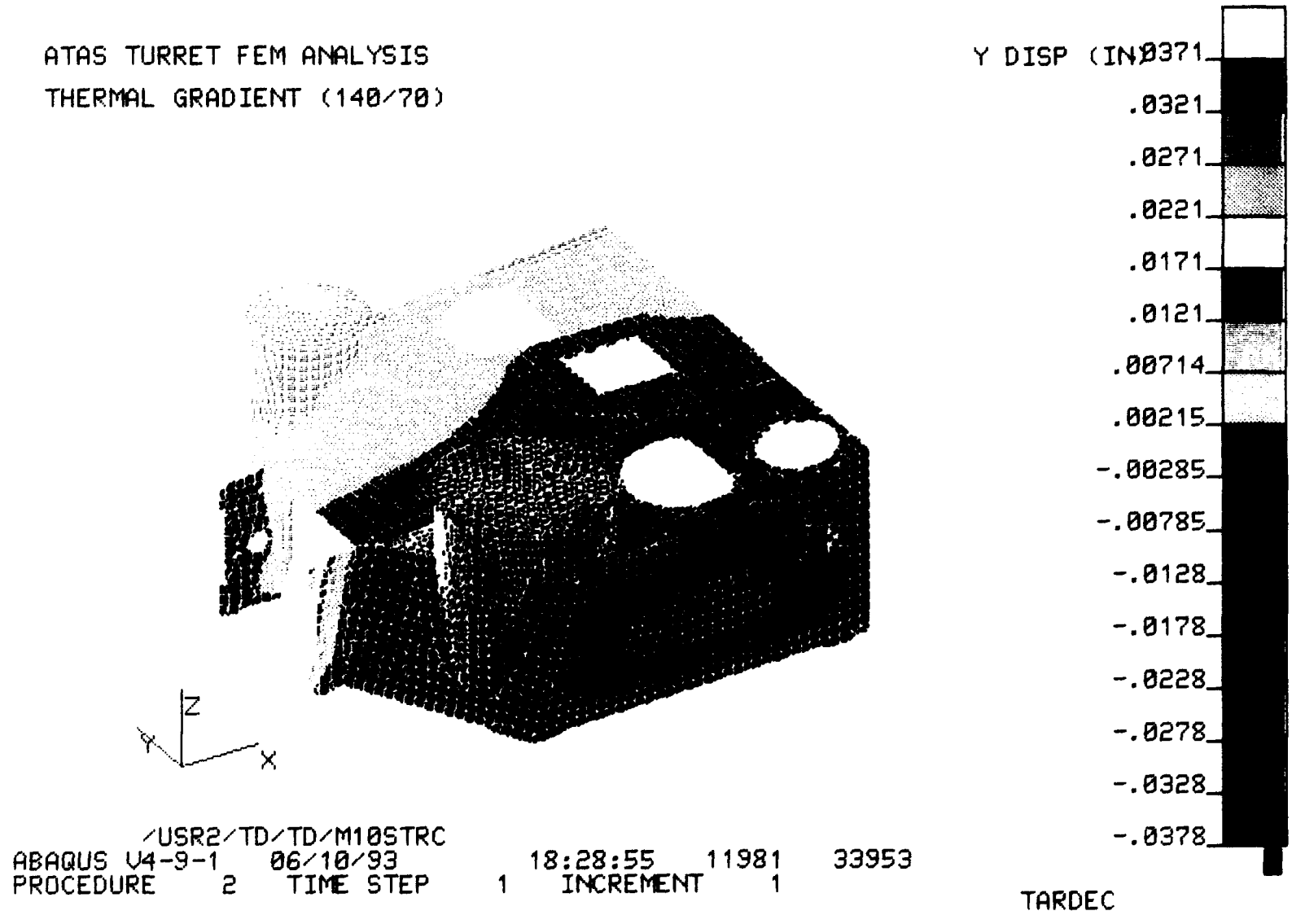

FIG 5-7 LATERAL DISPLACEMENT UNDER (140/70) THERMAL GRADIENT

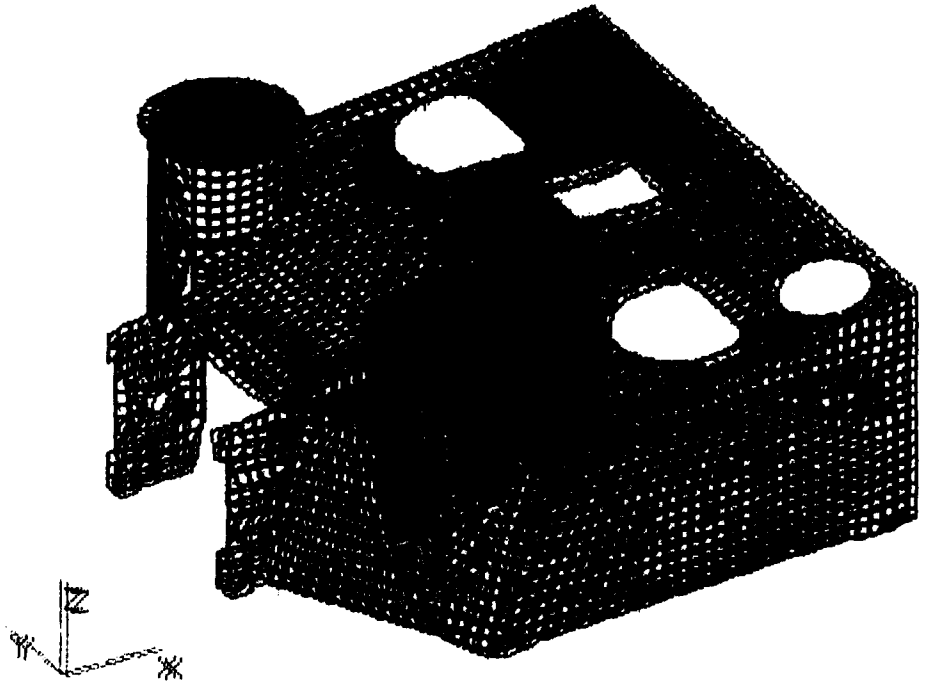

FIG.5-8 DEFORMED SHAPE FOR ATAS TURRET DUE TO (140/70) THERMAL GRADIENT

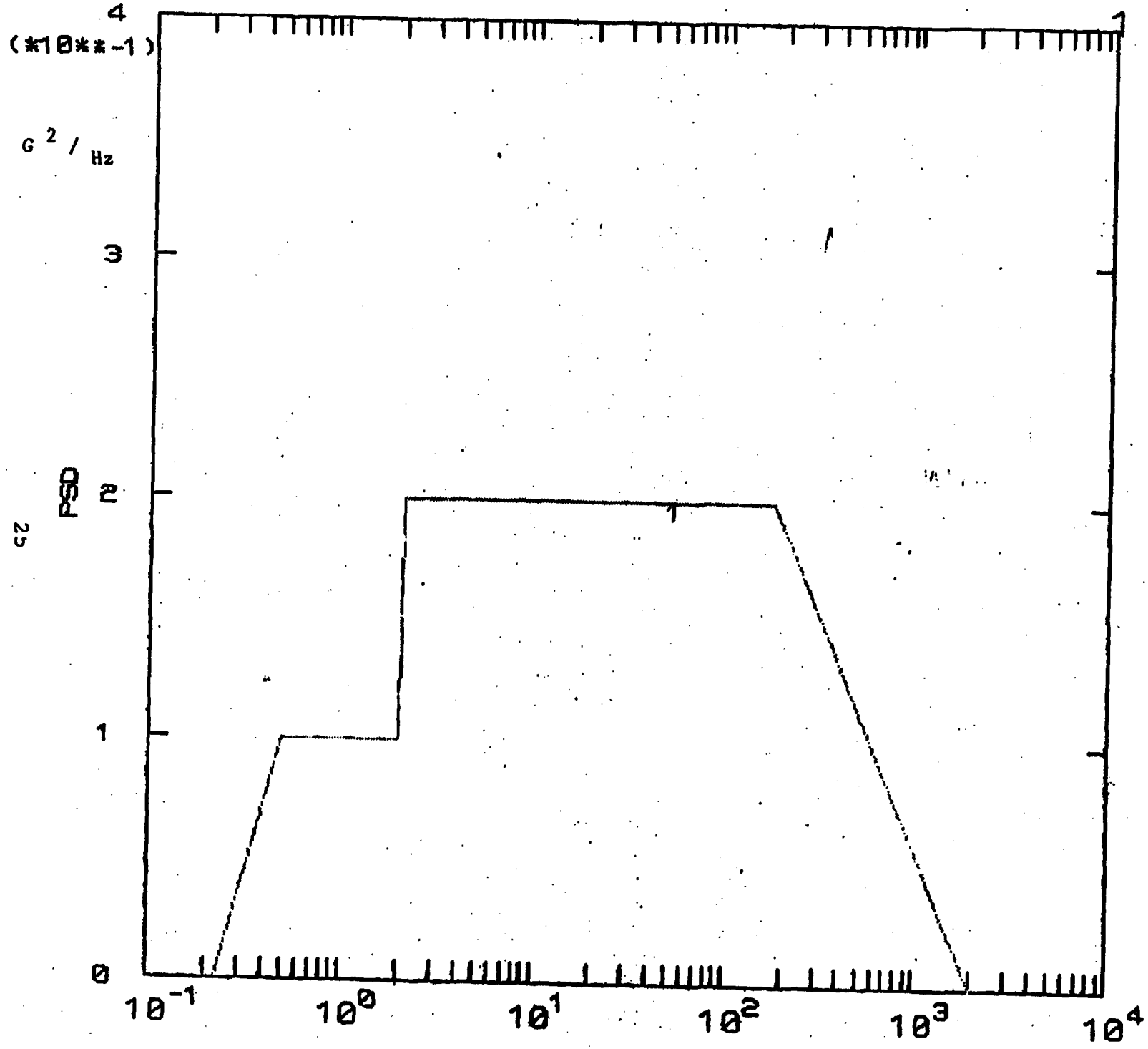

Fig. 6-1 BASE MOTION PSD

THE FIRST 10 EIGENVALUES HAVE CONVERGED

E I G E N V A L U E O U T P U T

MODE NO	EIGENVALUE	FREQUENCY (RAD/TIME)	FREQUENCY (CYCLES/TIME)	GENERALIZED MASS	COMPOSITE MODAL DAMPING
1	21499.	146.63	23.336	0.34706	0.00000E+00
2	74209.	272.41	43.356	0.48074	0.00000E+00
3	93367.	305.56	48.631	0.36200	0.00000E+00
4	1.11878E+05	334.48	53.235	0.15282	0.00000E+00
5	1.32168E+05	363.55	57.861	0.87563	0.00000E+00
6	1.59130E+05	398.91	63.489	0.86213	0.00000E+00
7	2.59575E+05	509.49	81.087	7.49876E-02	0.00000E+00
8	2.69242E+05	518.89	82.583	0.53931	0.00000E+00
9	3.02448E+05	549.95	87.528	2.8344	0.00000E+00
10	3.39704E+05	582.84	92.762	1.7214	0.00000E+00
11			99.6		
12			110		
13			116		
14			126		
15			141		
16			146		
17			149		
18			154		
19			10000		

FIG. 6-2 ATAS TURRET MODES AND THEIR FREQUENCIES

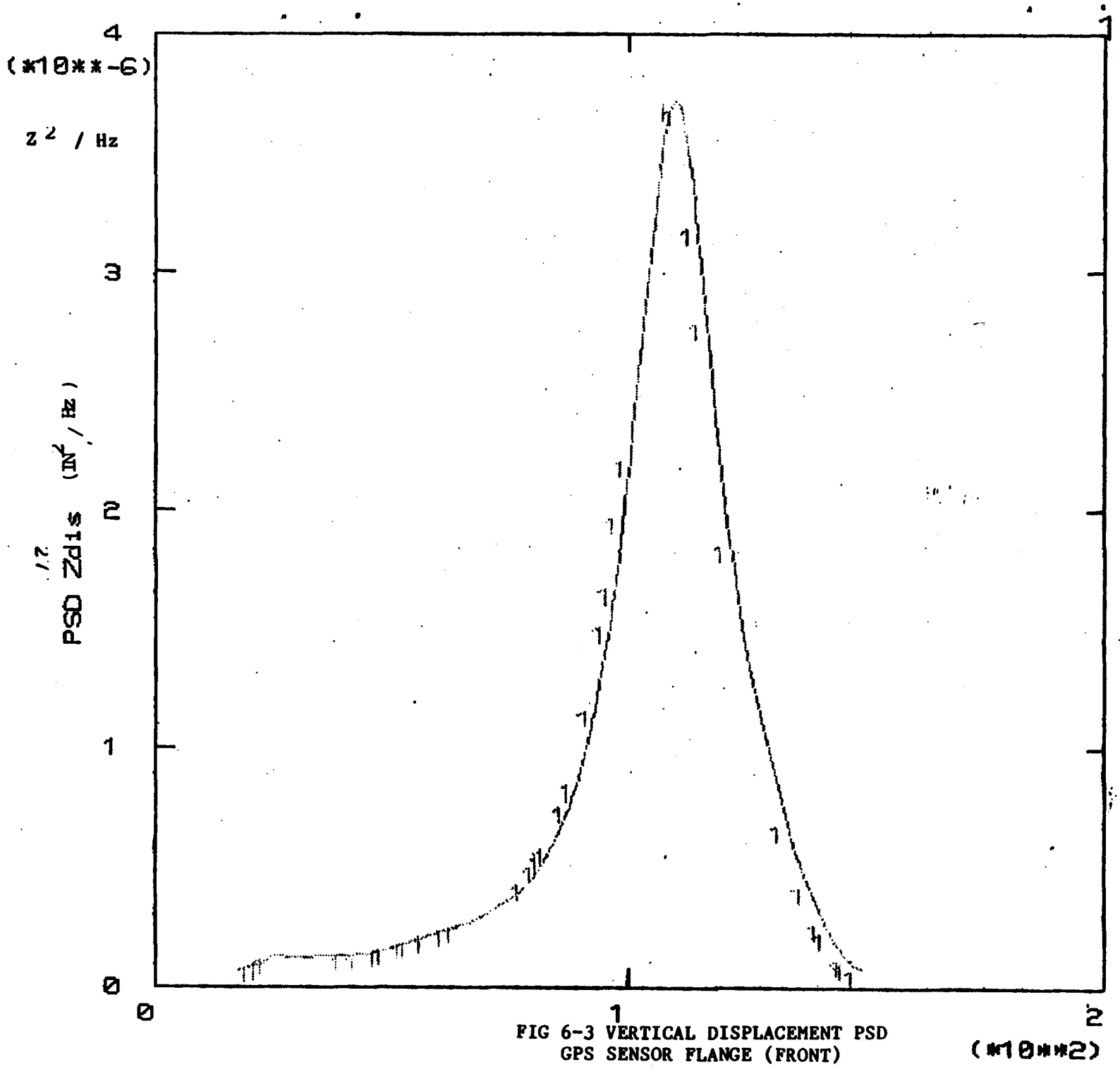

FIG 6-3 VERTICAL DISPLACEMENT PSD
GPS SENSOR FLANGE (FRONT)

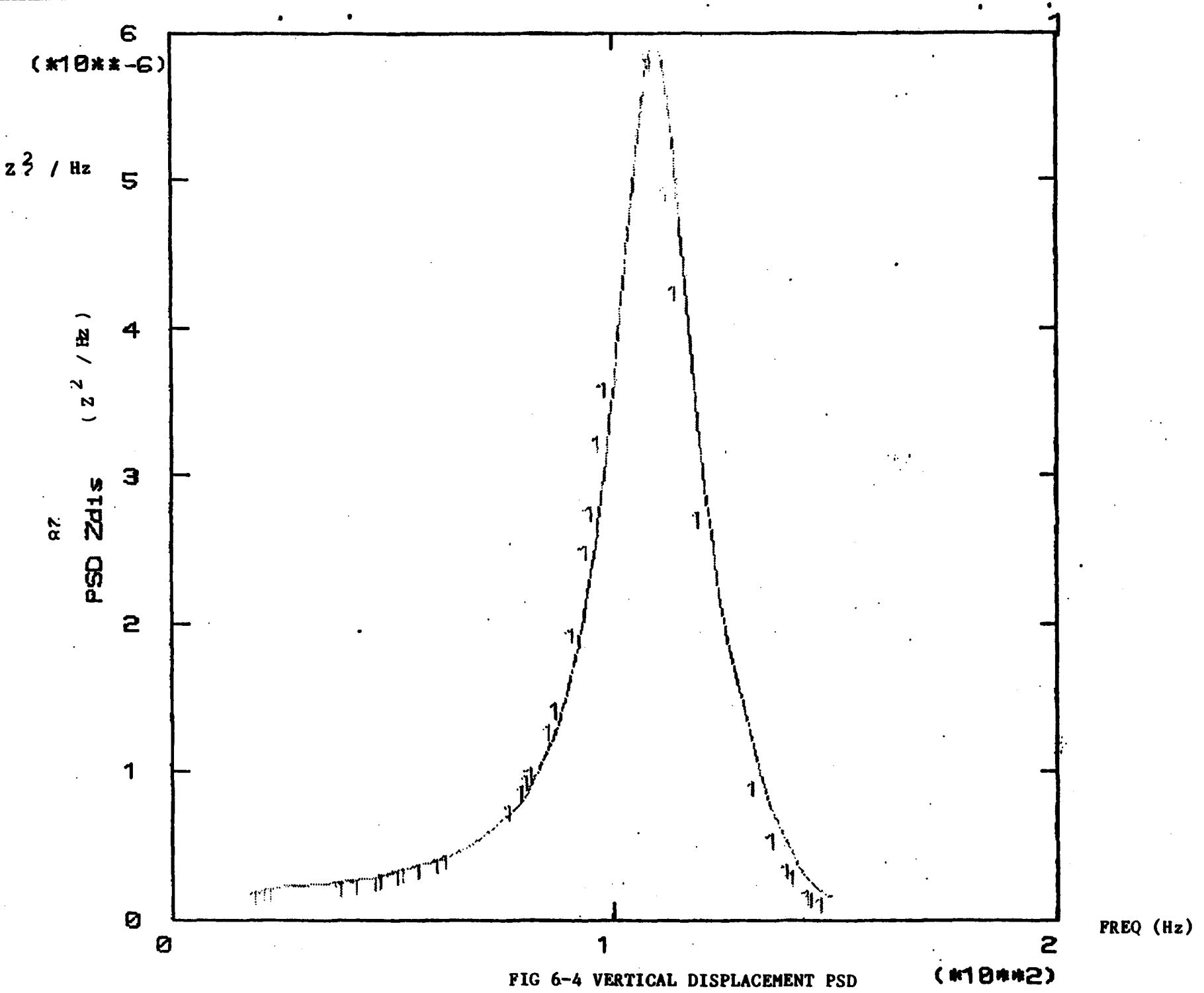

FIG 6-4 VERTICAL DISPLACEMENT PSD
GPS SENSOR FLANGE (RIGHT)

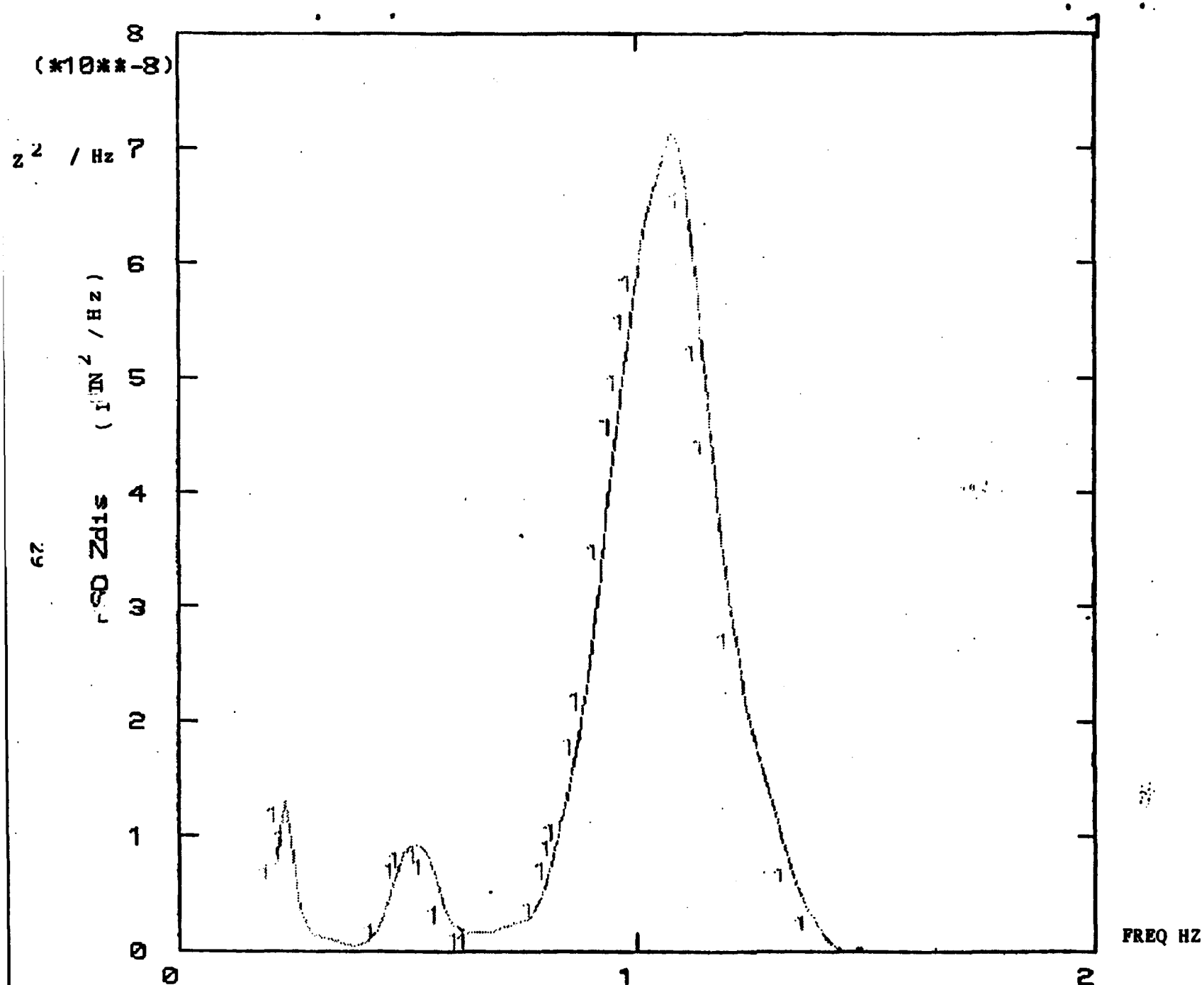

FIG 6-5 VERTICAL DISPLACEMENT PSD
GPS SENSOR FLANGE (REAR)

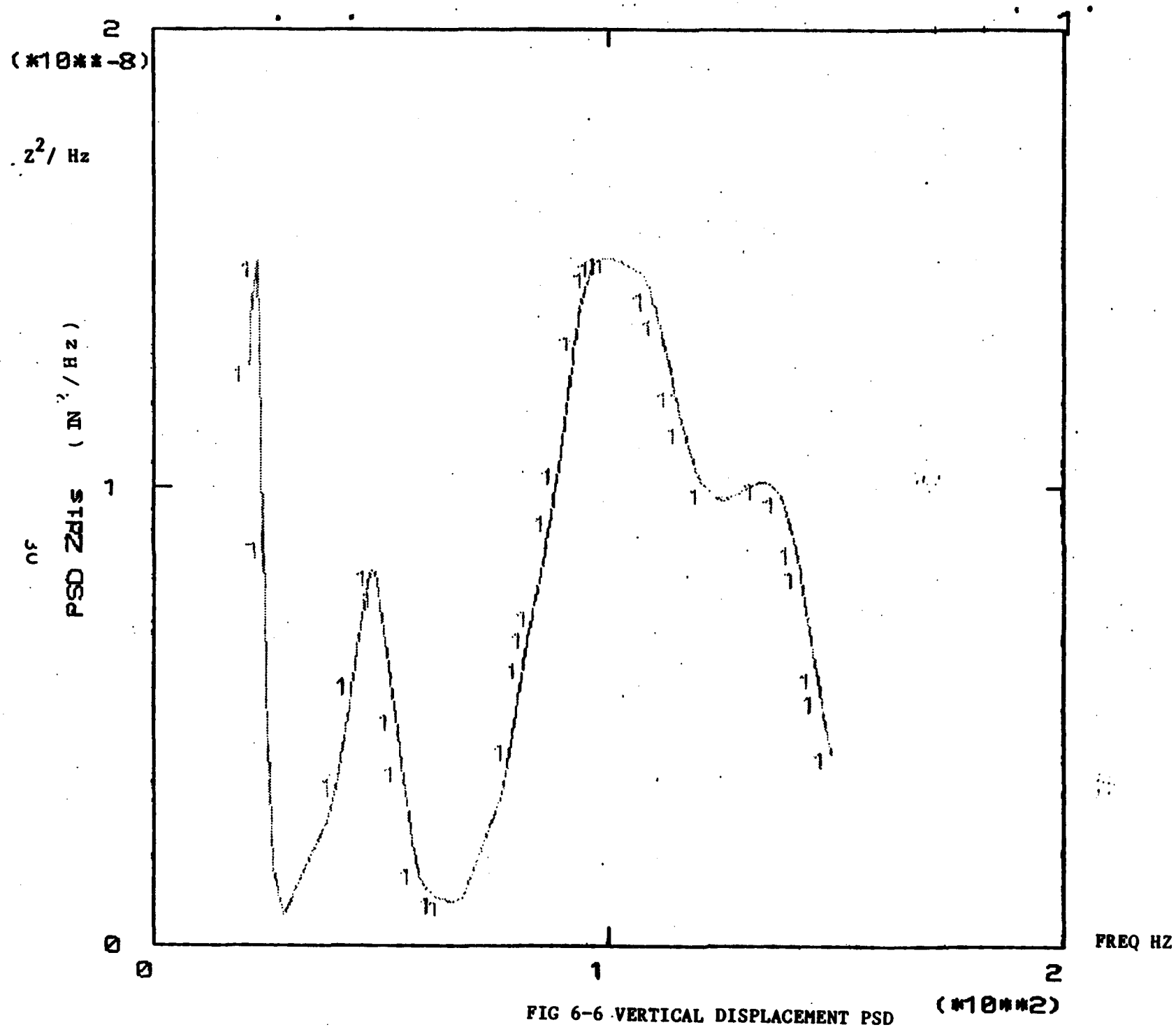

FIG 6-6 VERTICAL DISPLACEMENT PSD
GPS SENSOR FLANGE (LEFT)

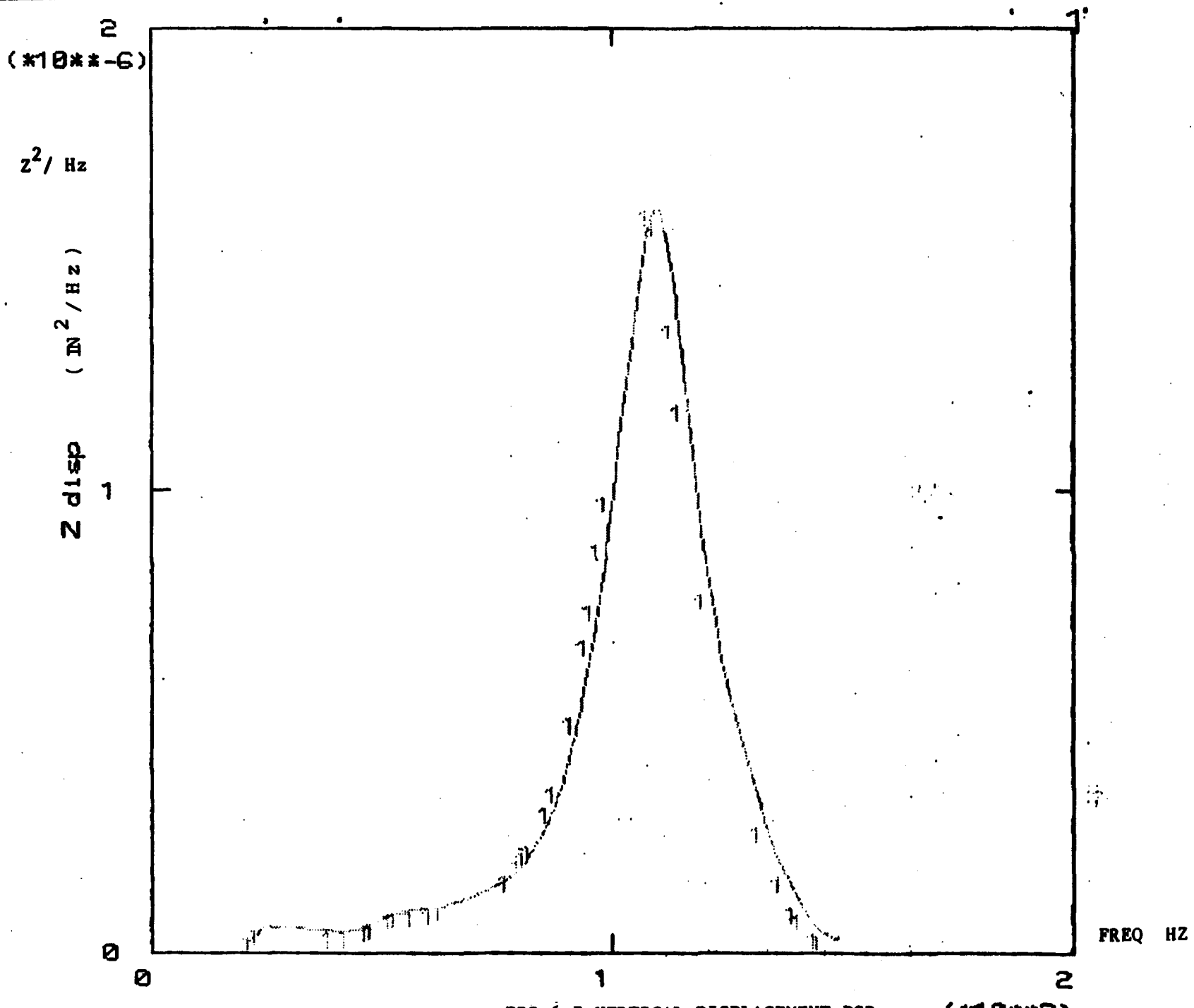

FIG 6-7 VERTICAL DISPLACEMENT PSD
GPS COVER PLATE (CENTER)

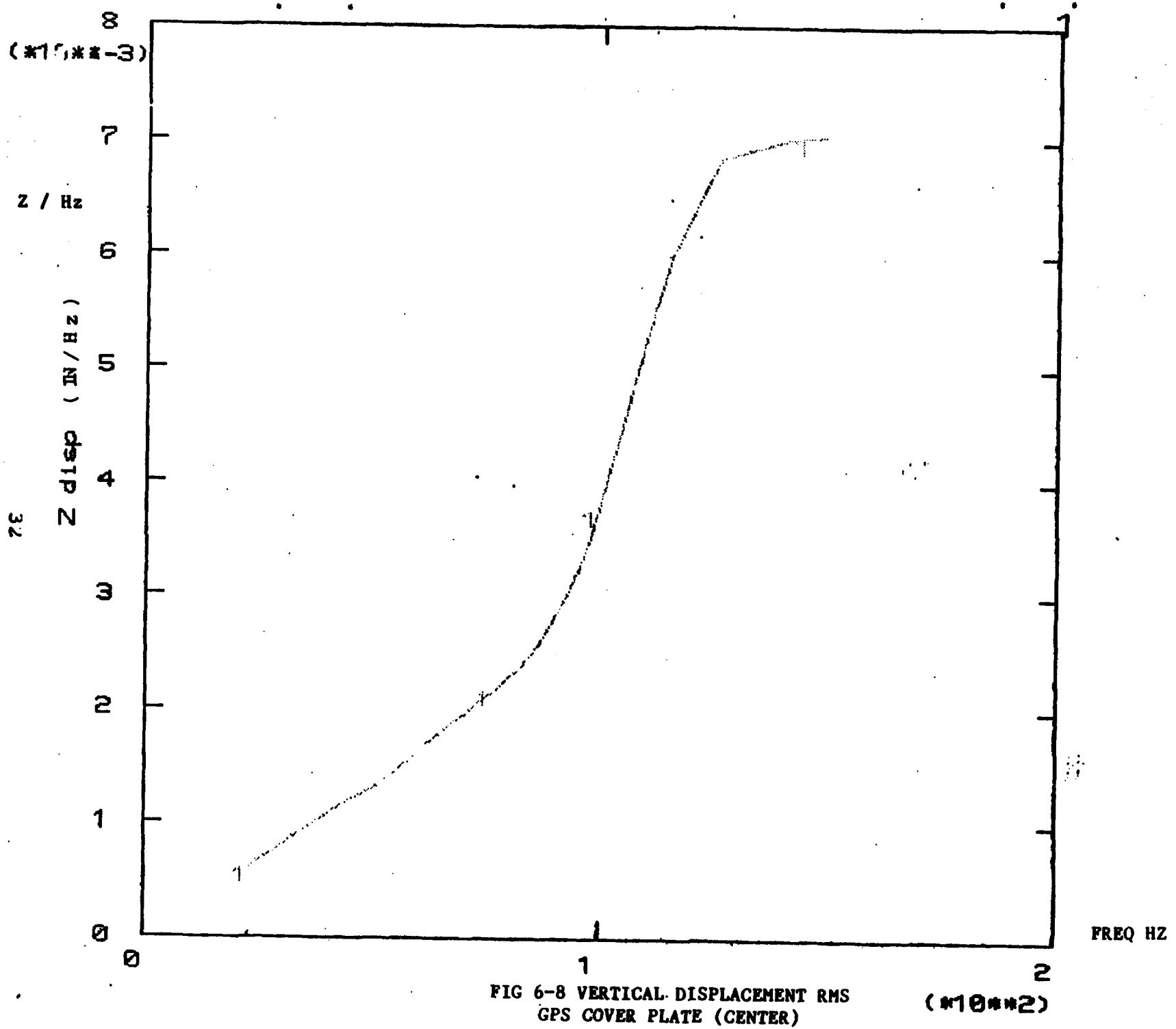

FIG 6-8 VERTICAL DISPLACEMENT RMS
GPS COVER PLATE (CENTER)

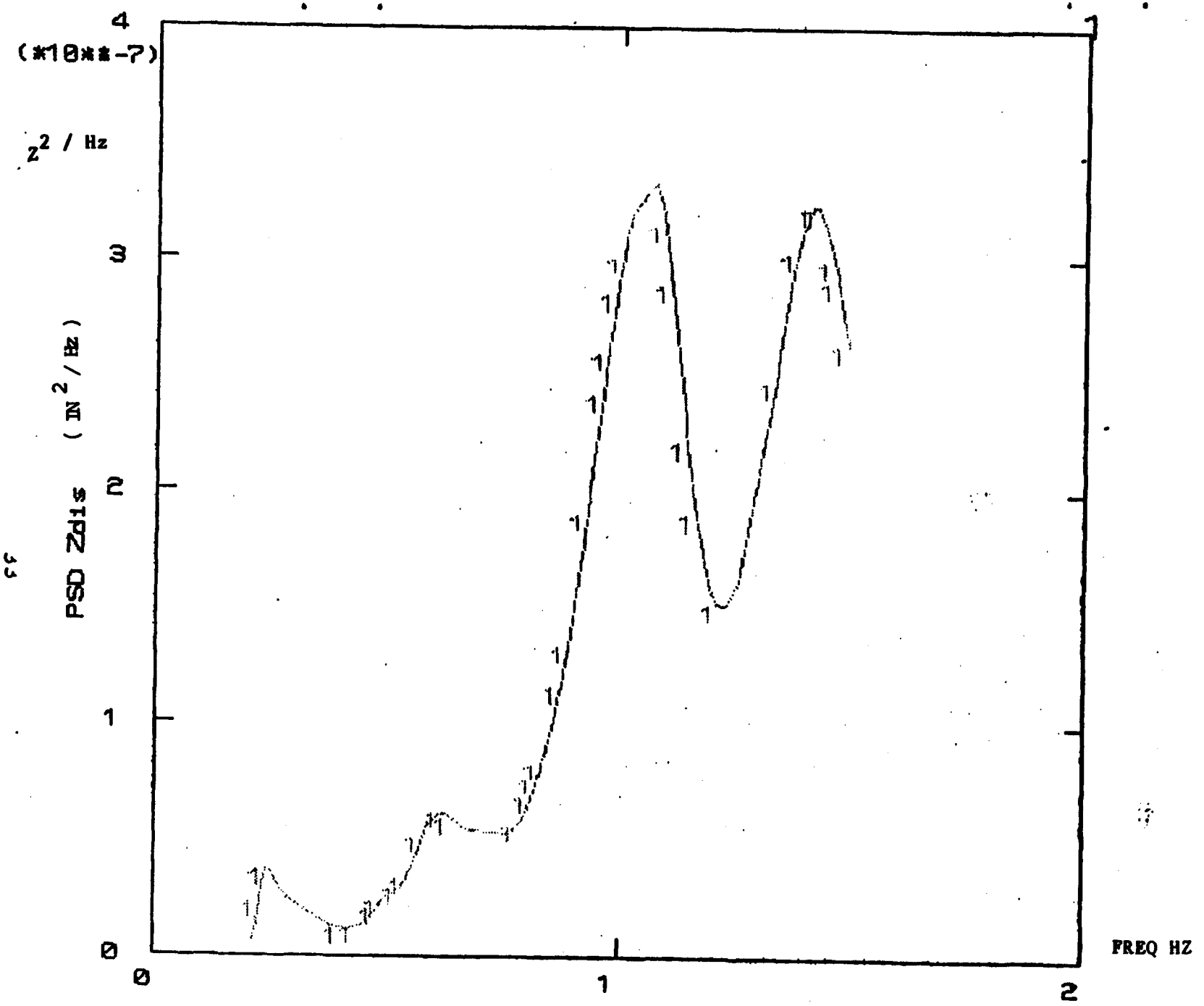

FIG 6-9 VERTICAL DISPLACEMENT PSD
SGTS SENSOR FLANGE (FRONT)

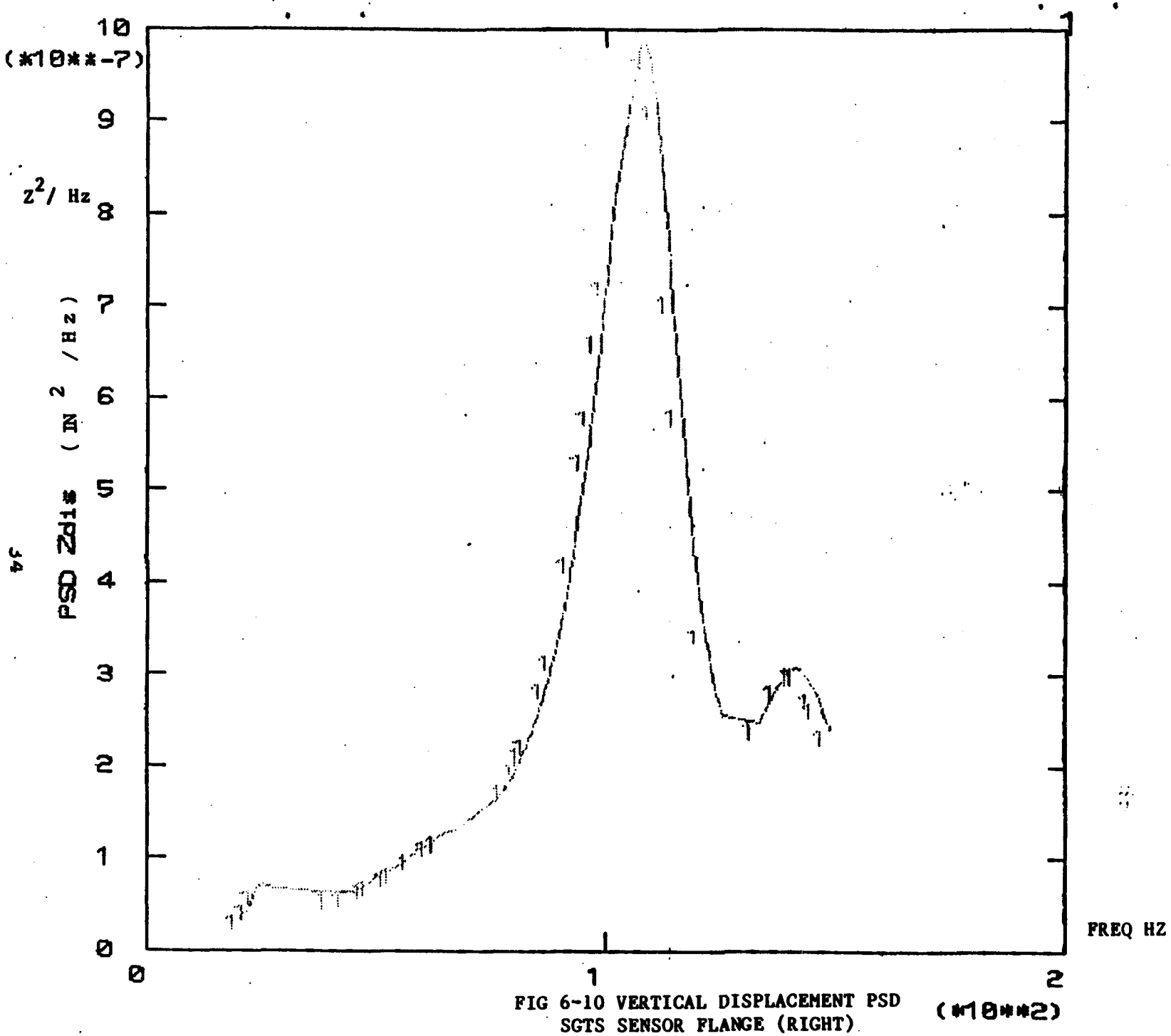

FIG 6-10 VERTICAL DISPLACEMENT PSD
SGTS SENSOR FLANGE (RIGHT)

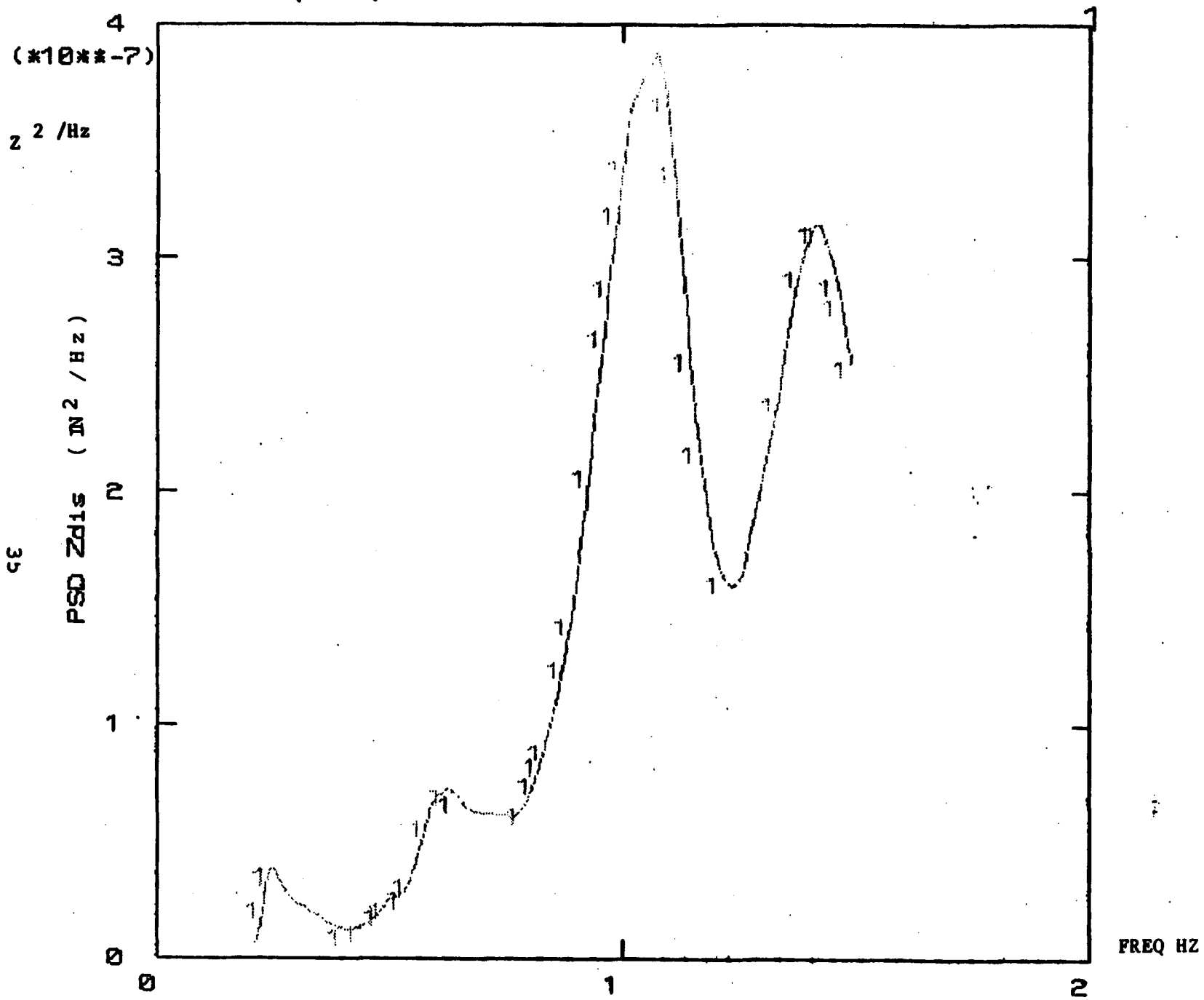

FIG 6-11 VERTICAL DISPLACEMENT PSD
SGTS SENSOR FLANGE (REAR)

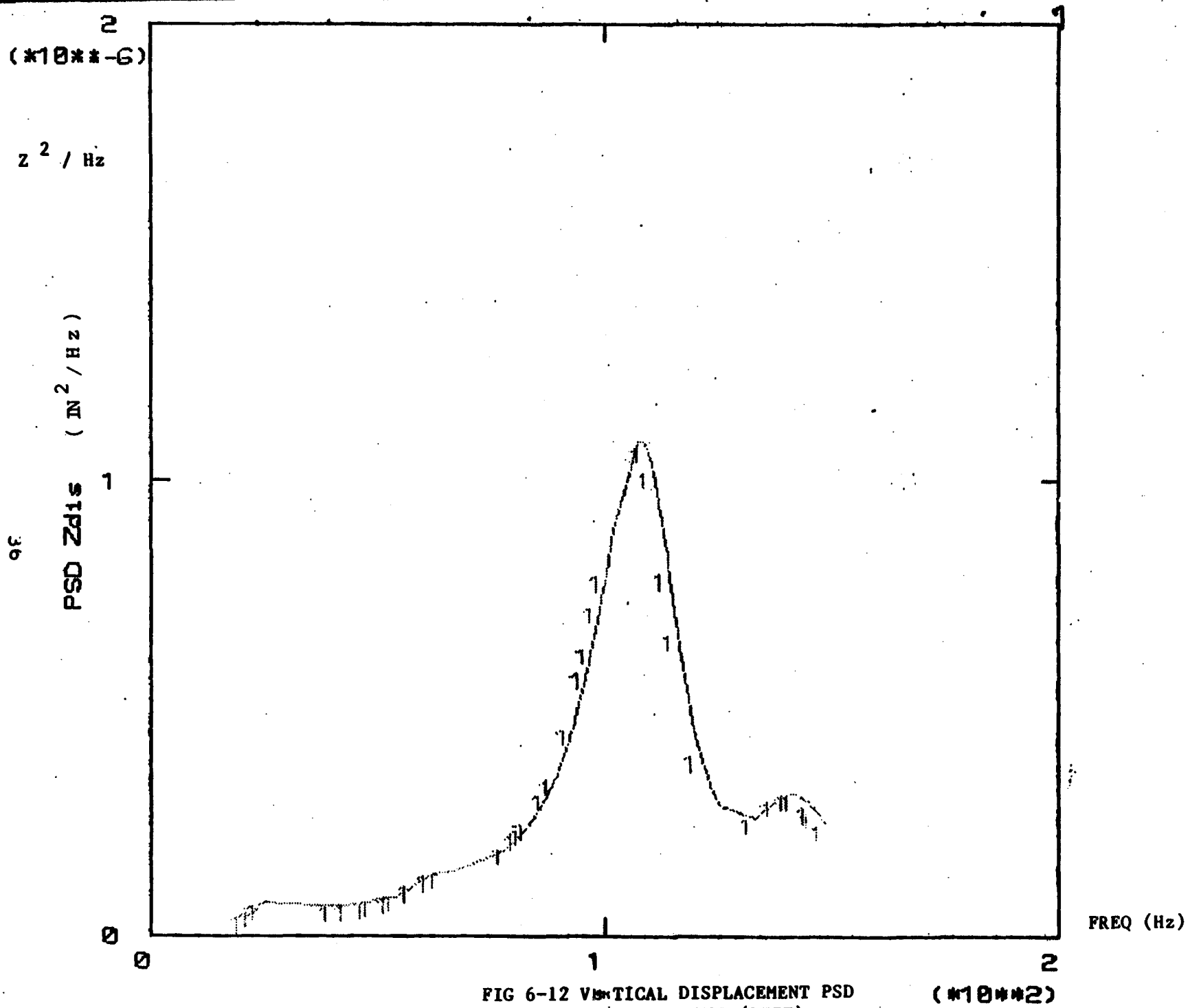

FIG 6-12 VERTICAL DISPLACEMENT PSD
SGTS SENSOR FLANGE (LEFT)

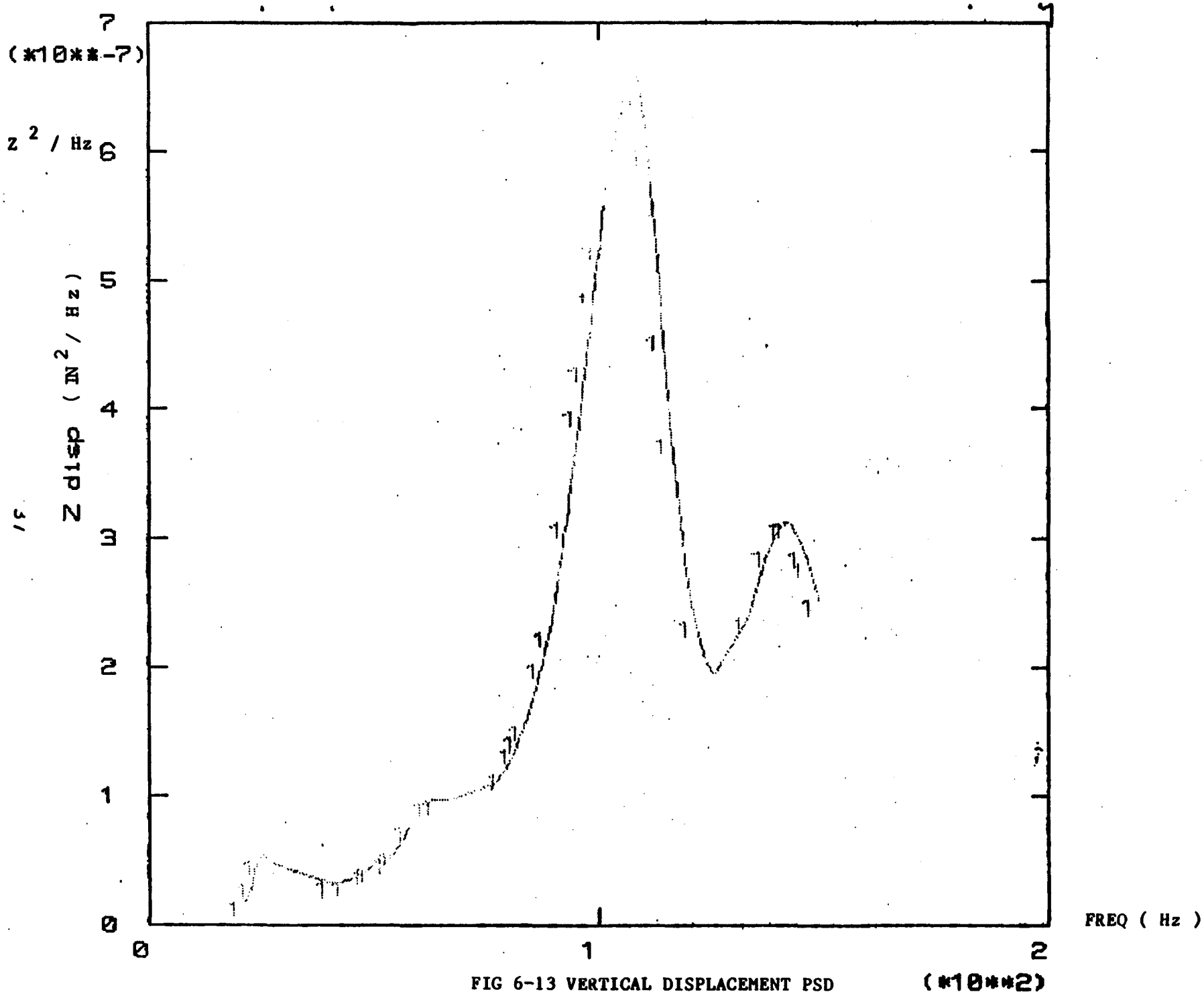

FIG 6-13 VERTICAL DISPLACEMENT PSD
SGTS COVER PLATE (CENTER)

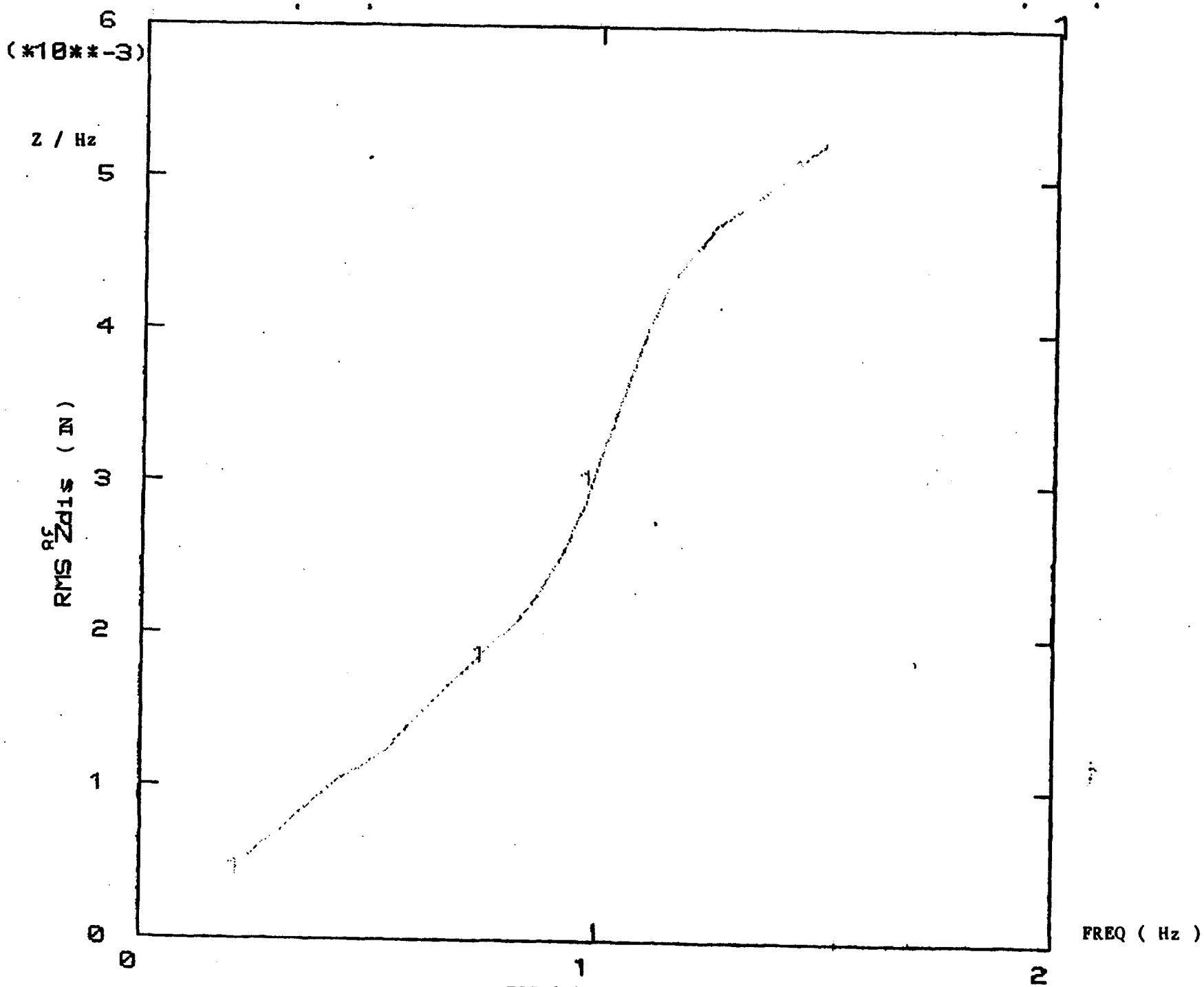

FIG 6-14 VERTICAL DISPLACEMENT RMS
SGTS COVER PLATE (CENTER)

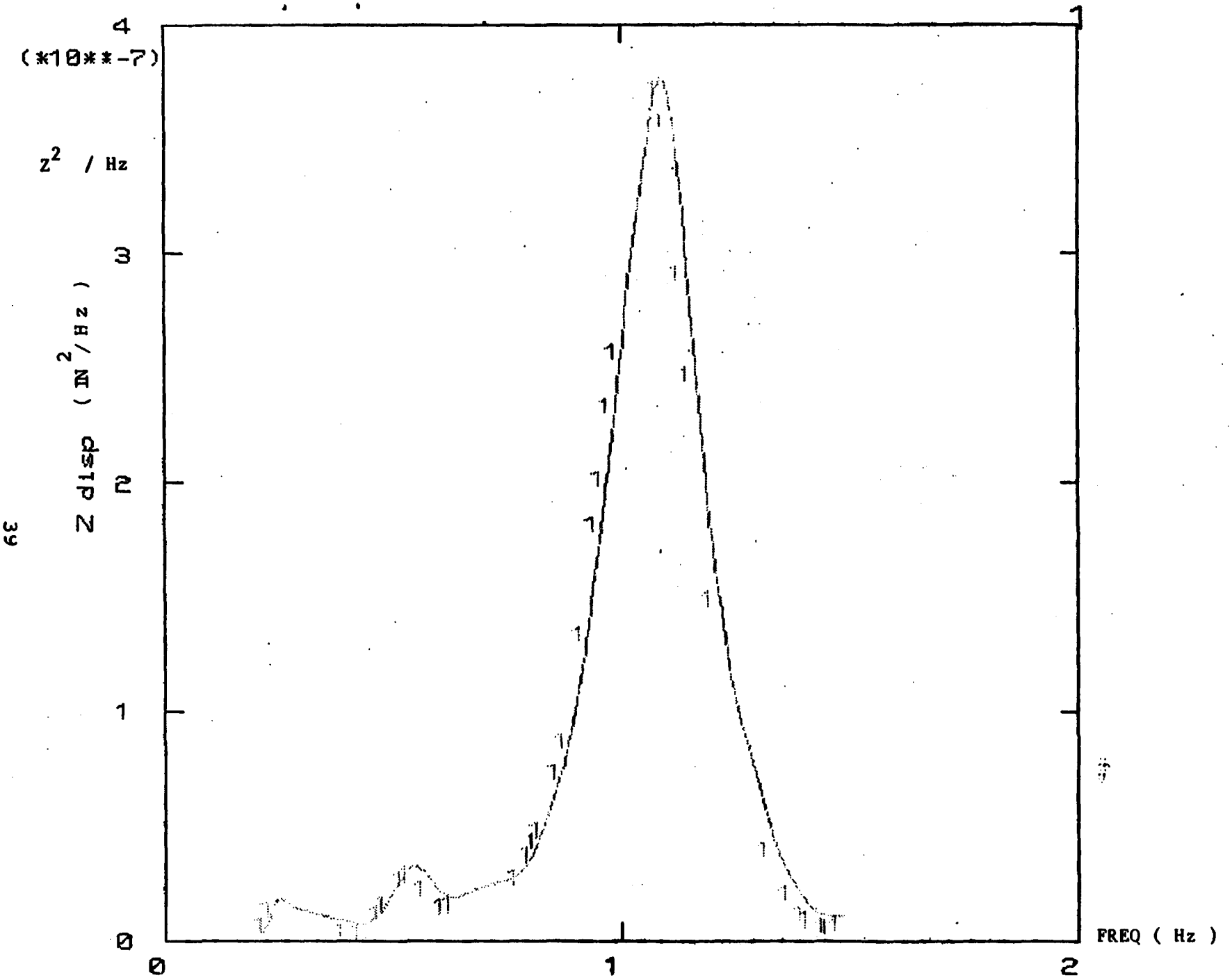

FIG 6-15 VERTICAL DISPLACEMENT PSD
LEFT TRUNNION

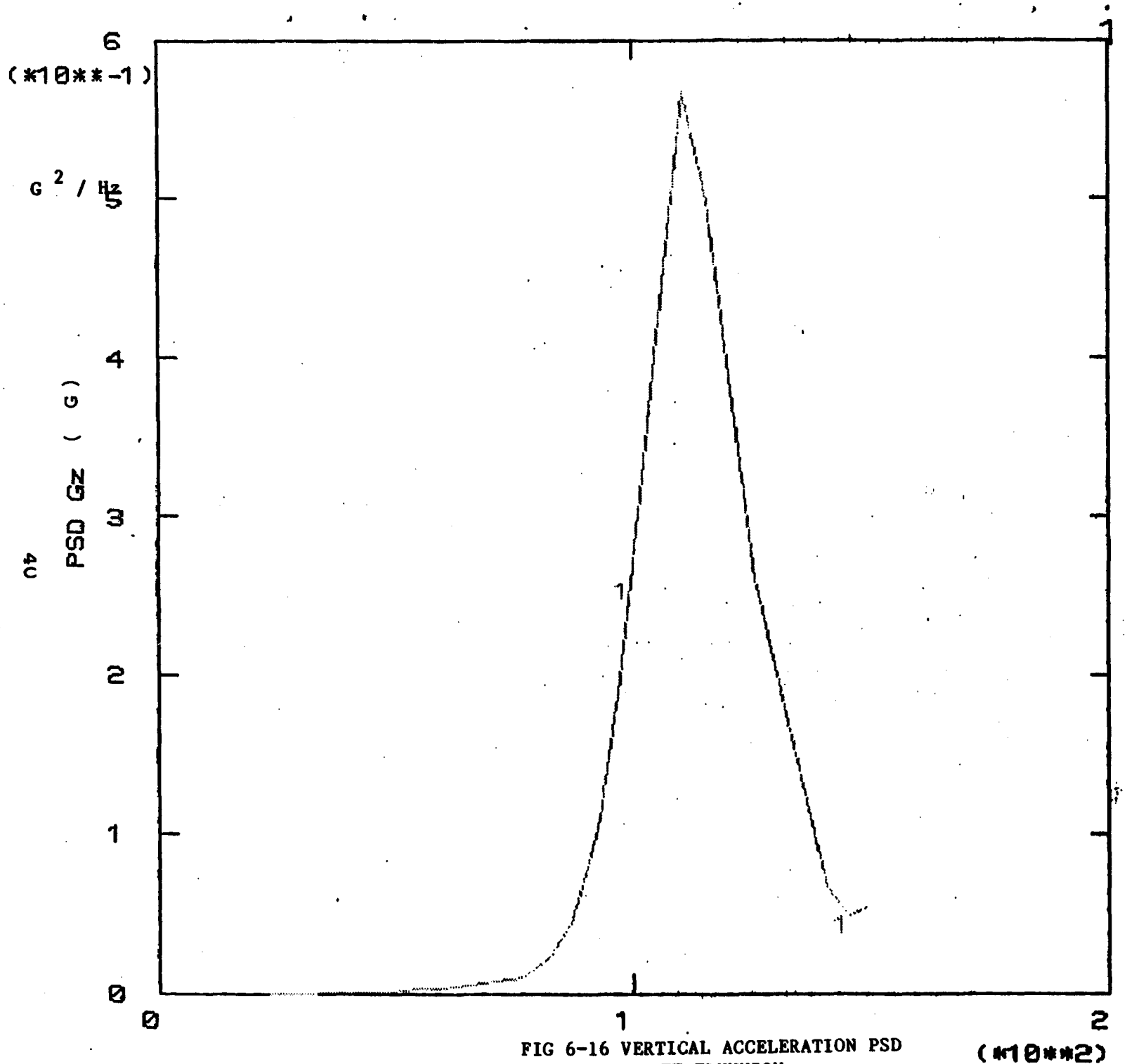

FIG 6-16 VERTICAL ACCELERATION PSD
LEFT TRUNNION

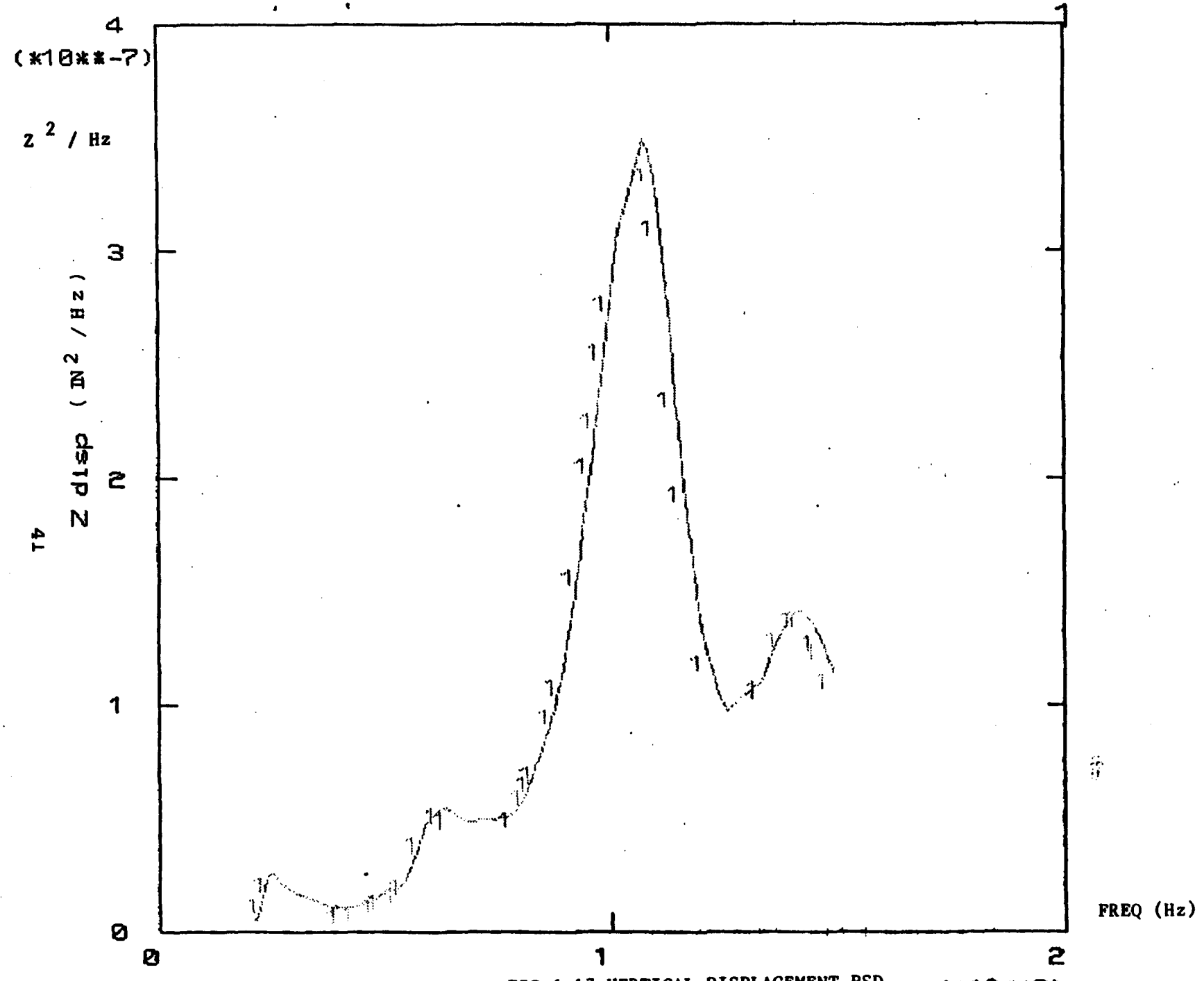

FIG 6-17 VERTICAL DISPLACEMENT PSD
RIGHT TRUNNION

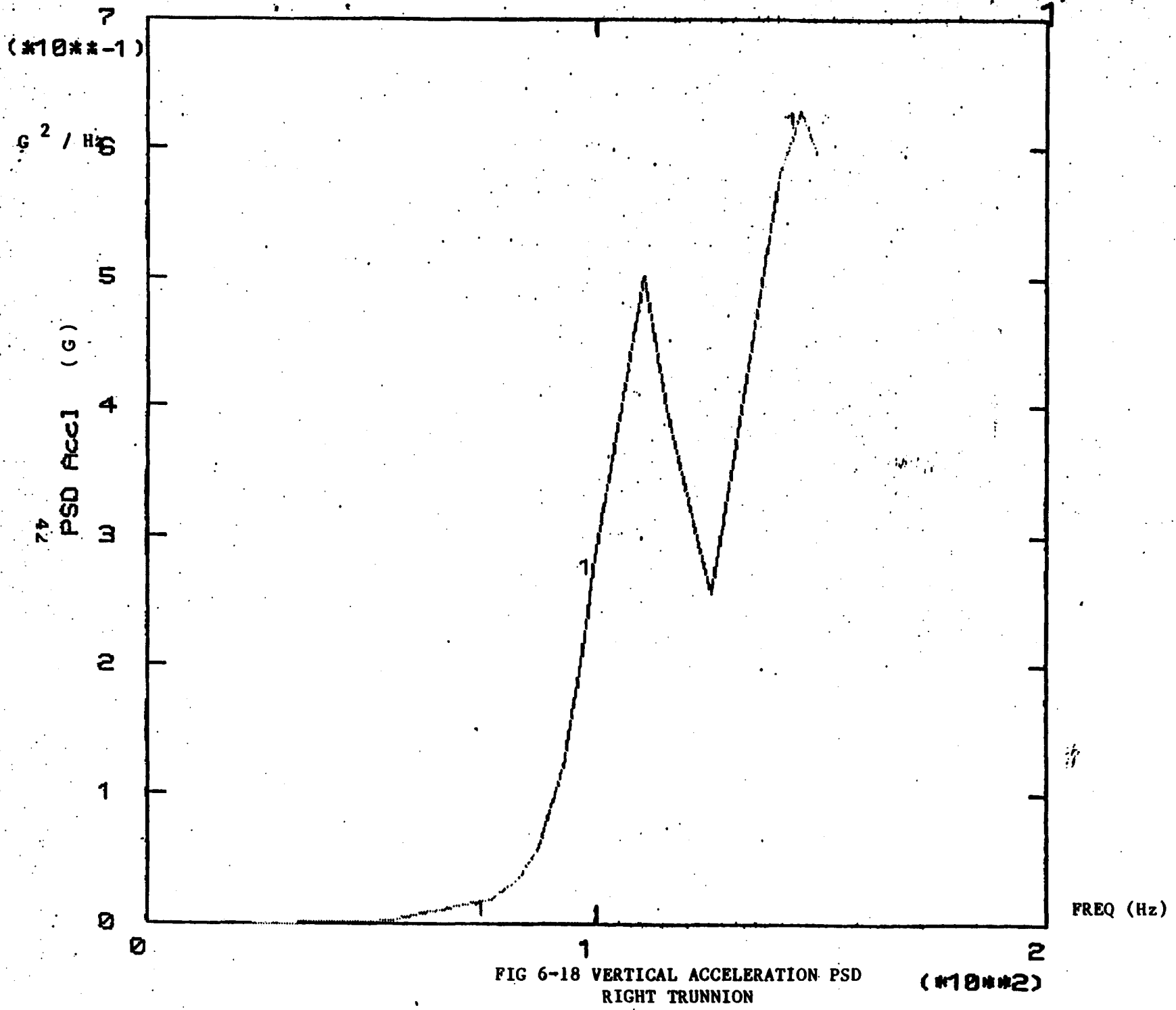

FIG 6-18 VERTICAL ACCELERATION PSD
RIGHT TRUNNION

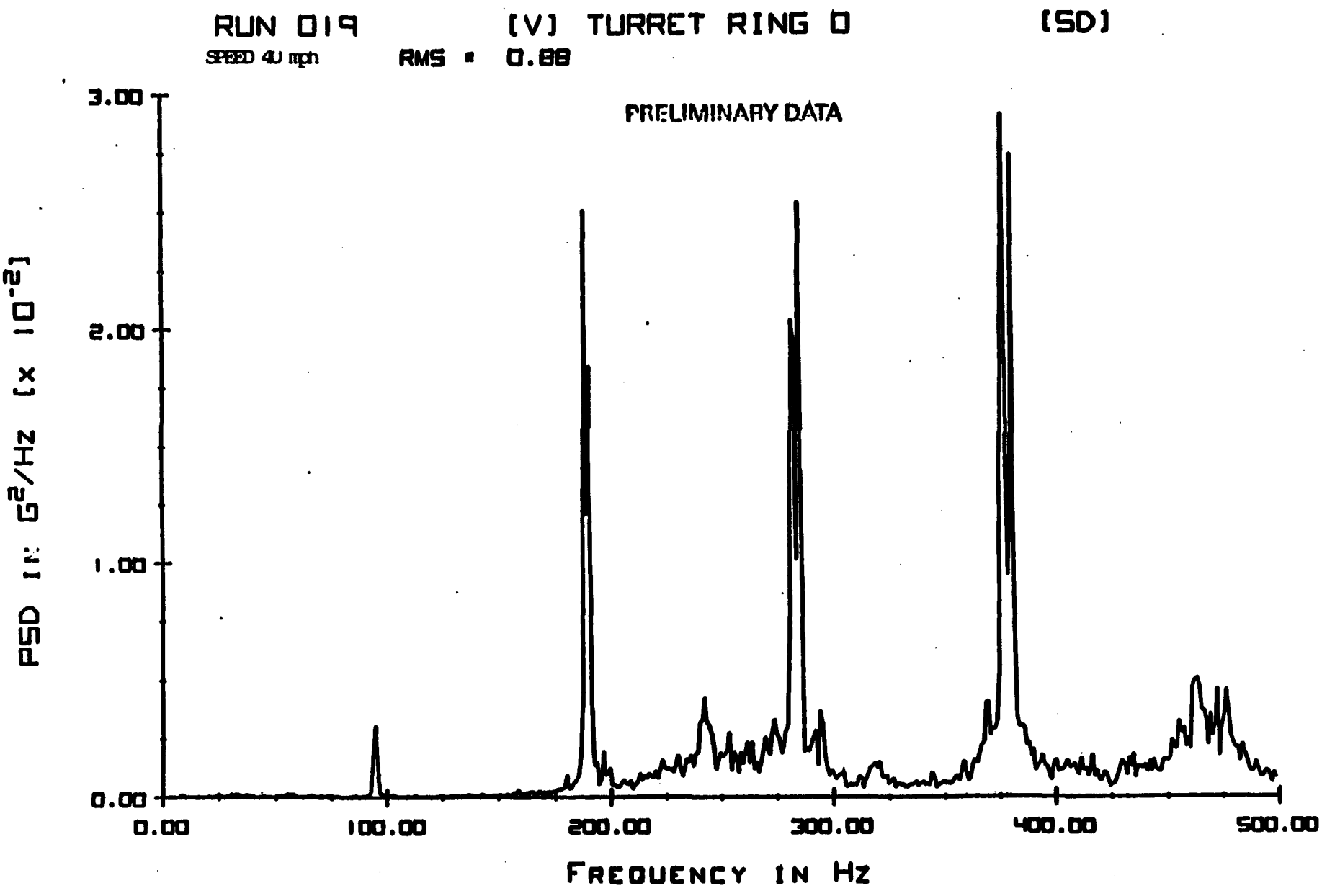

FIG 6-19 VERTICAL ACCELERATION PSD AT FRONT OF TURRET RING
TURRET IN NORMAL POSITION

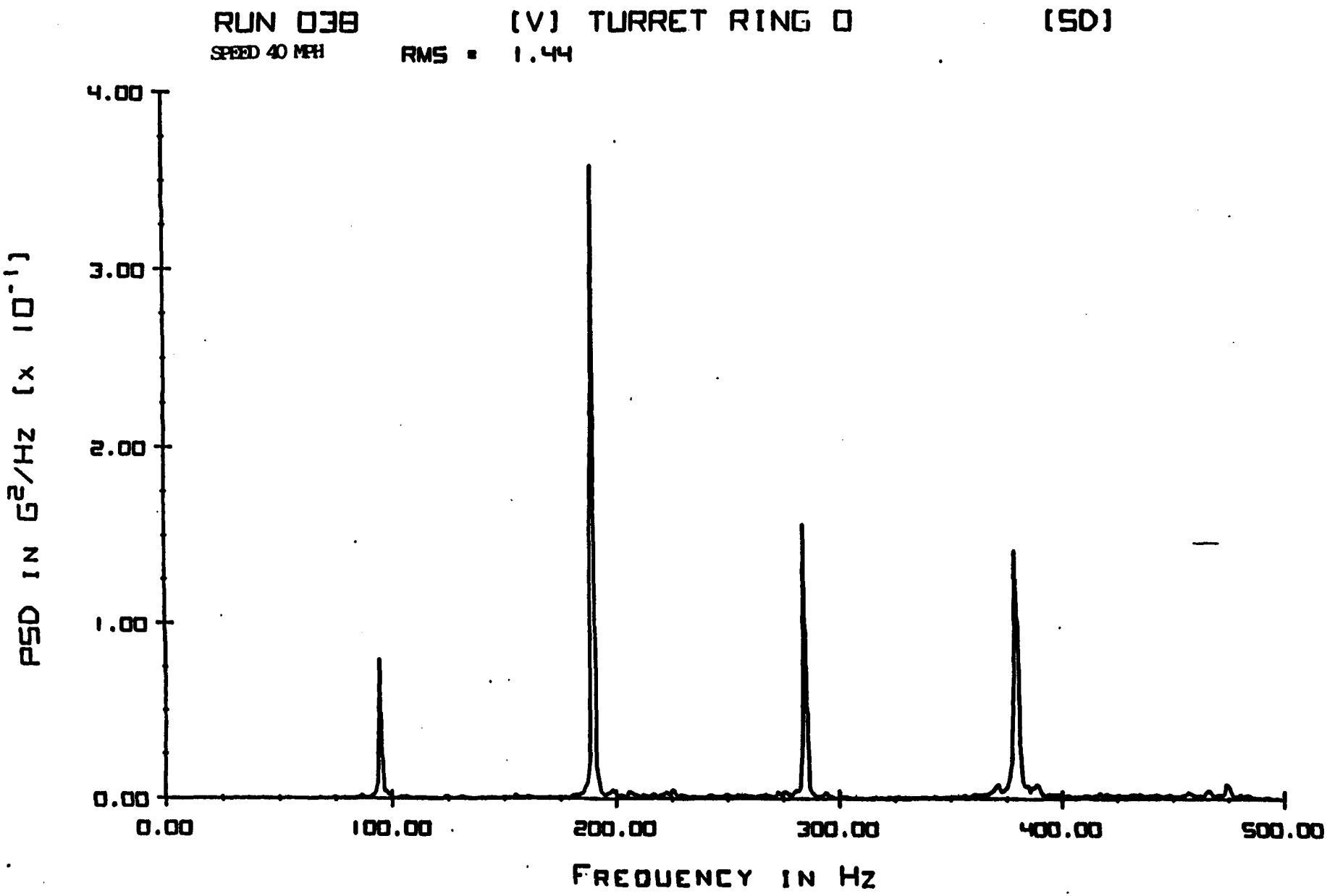

FIG 6-20 VERTICAL ACCELERATION PSD AT FRONT OF TURRET RING
TURRET ROTATED 90 DEG.

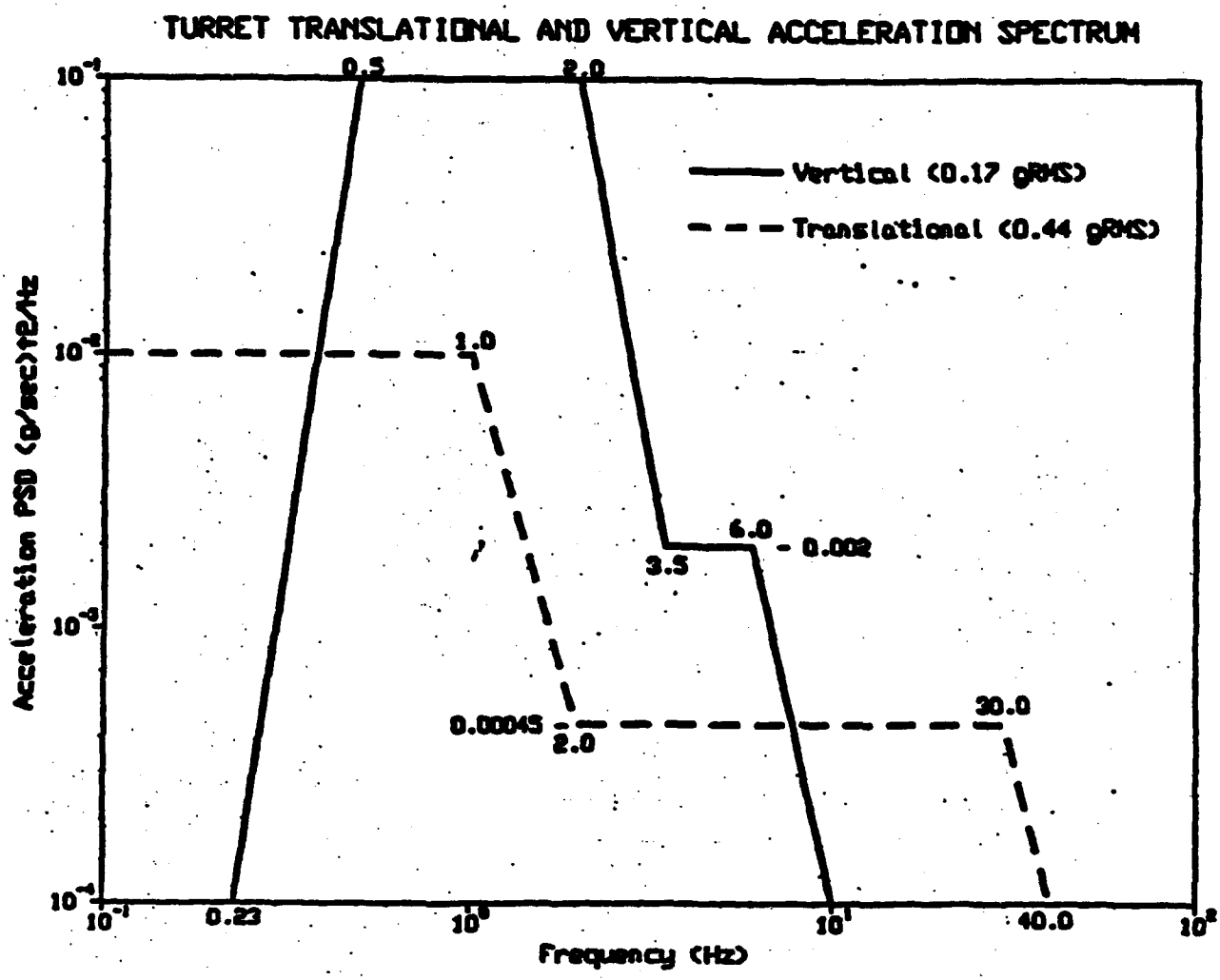

Fig. 6-21 VERTICAL ACCELERATION PSD FOR TURRET RING (LOW FREQUENCY)

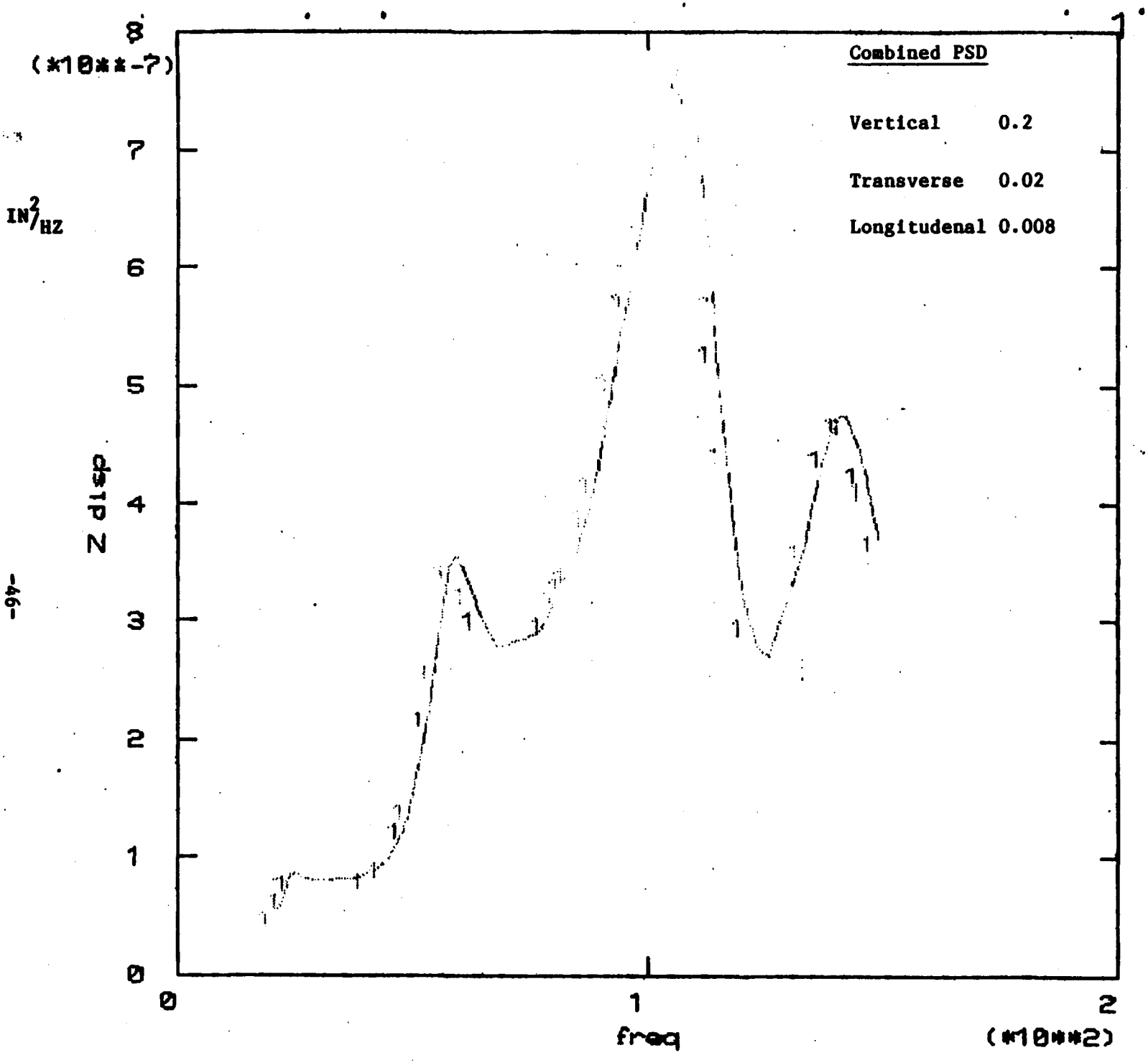

Fig 6.22 Vertical displacement at center CPS sensor under combined PSD

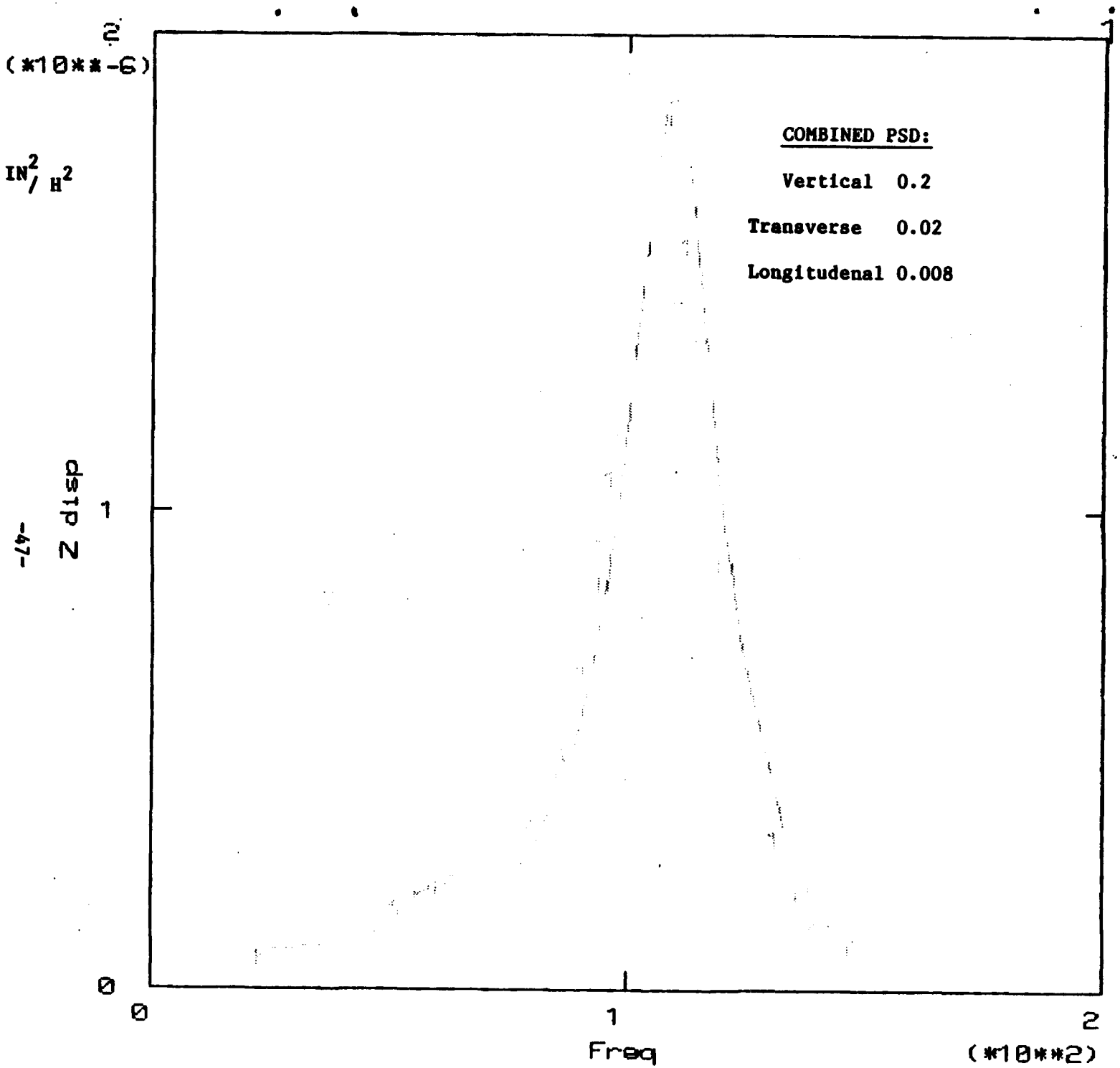

Fig 6.23 Vertical displacement at center of sets sensor under combined PSD

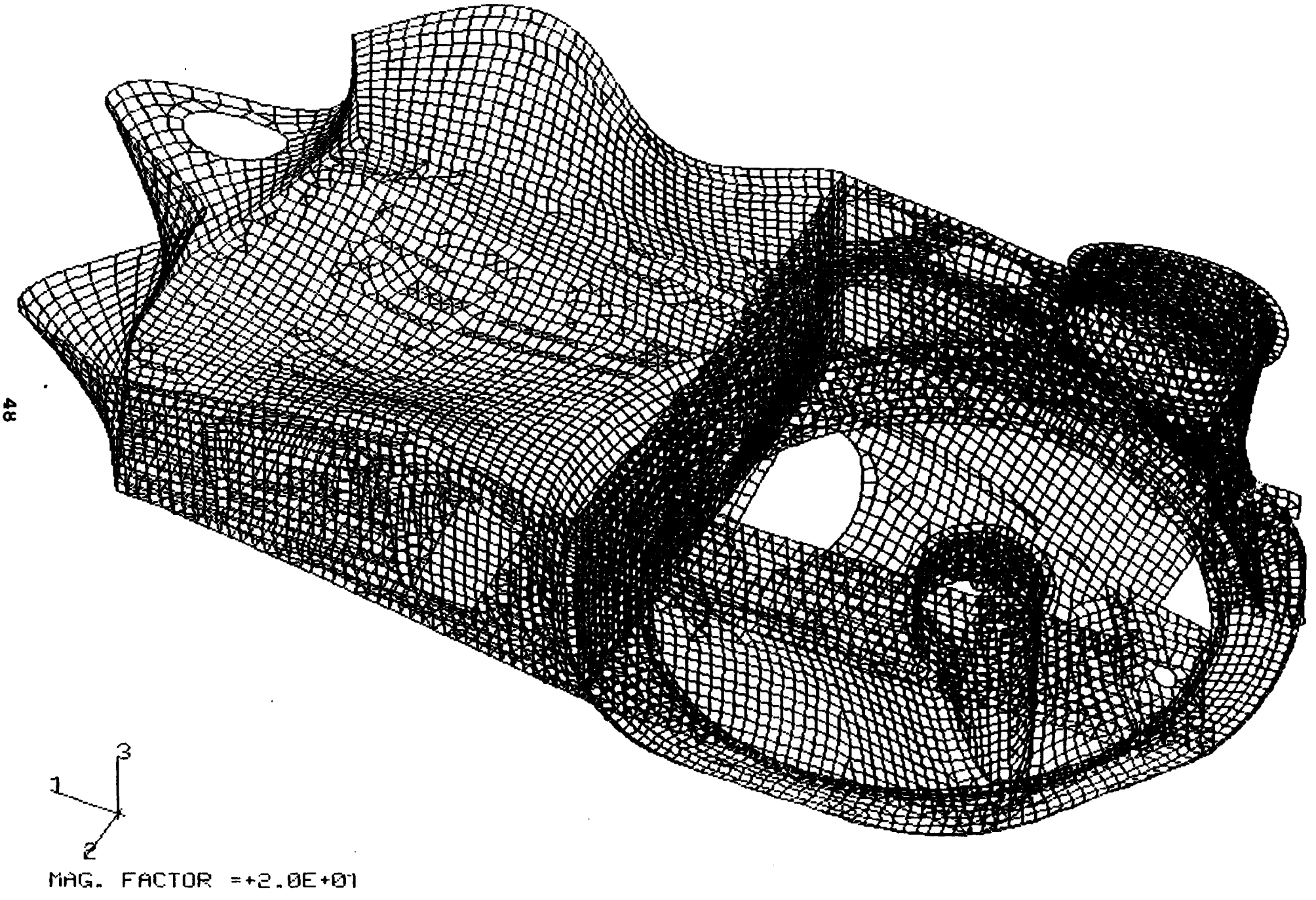

FIG.6-24 DEFORMED SHAPE FOR MODE NO 13 (FREQUENCY = 116 HZ)

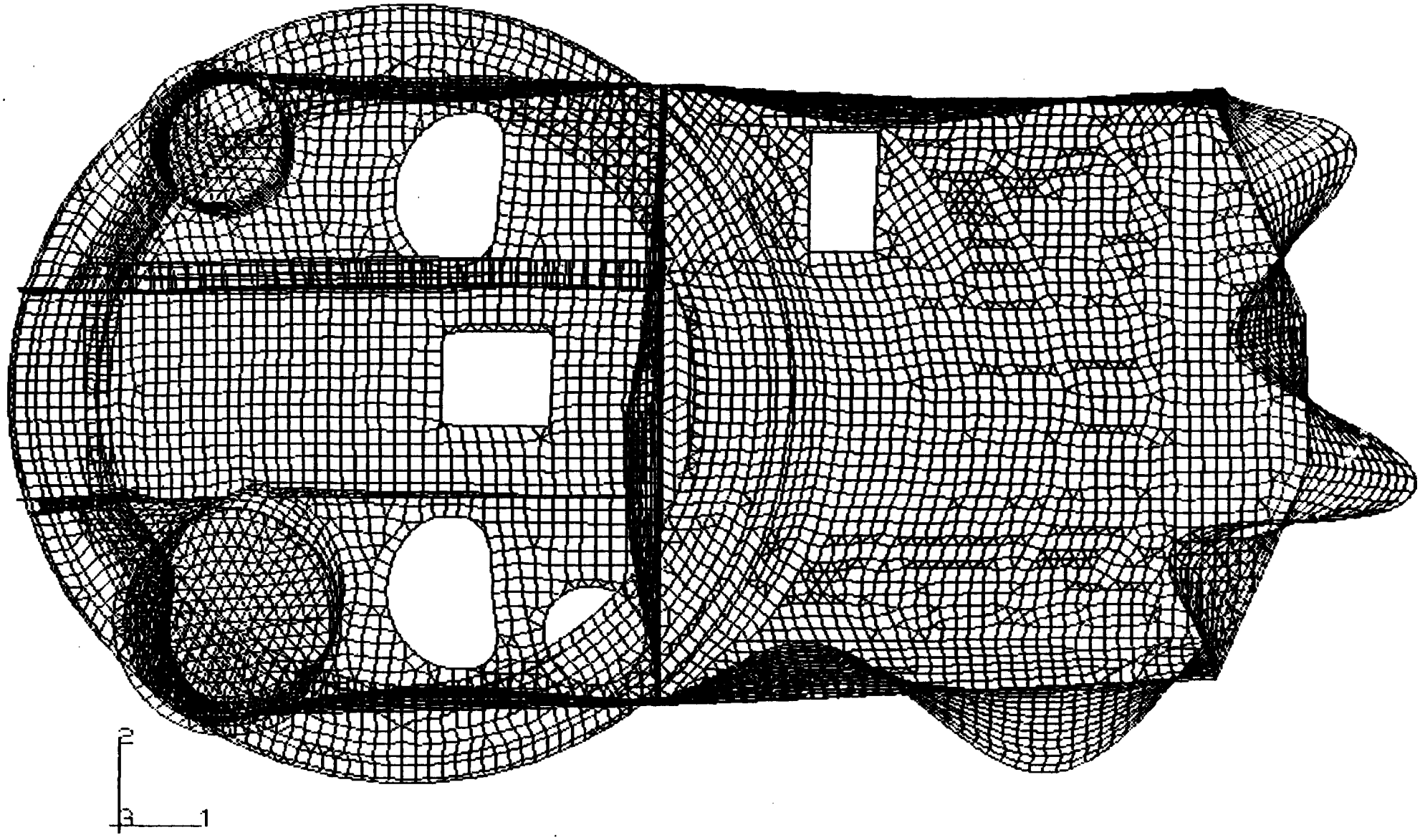

MAG. FACTOR =+2.0E+01

FIG 6-25 DEFORMED SHAPE FOR MODE 13 (FREQ = 116 Hz)

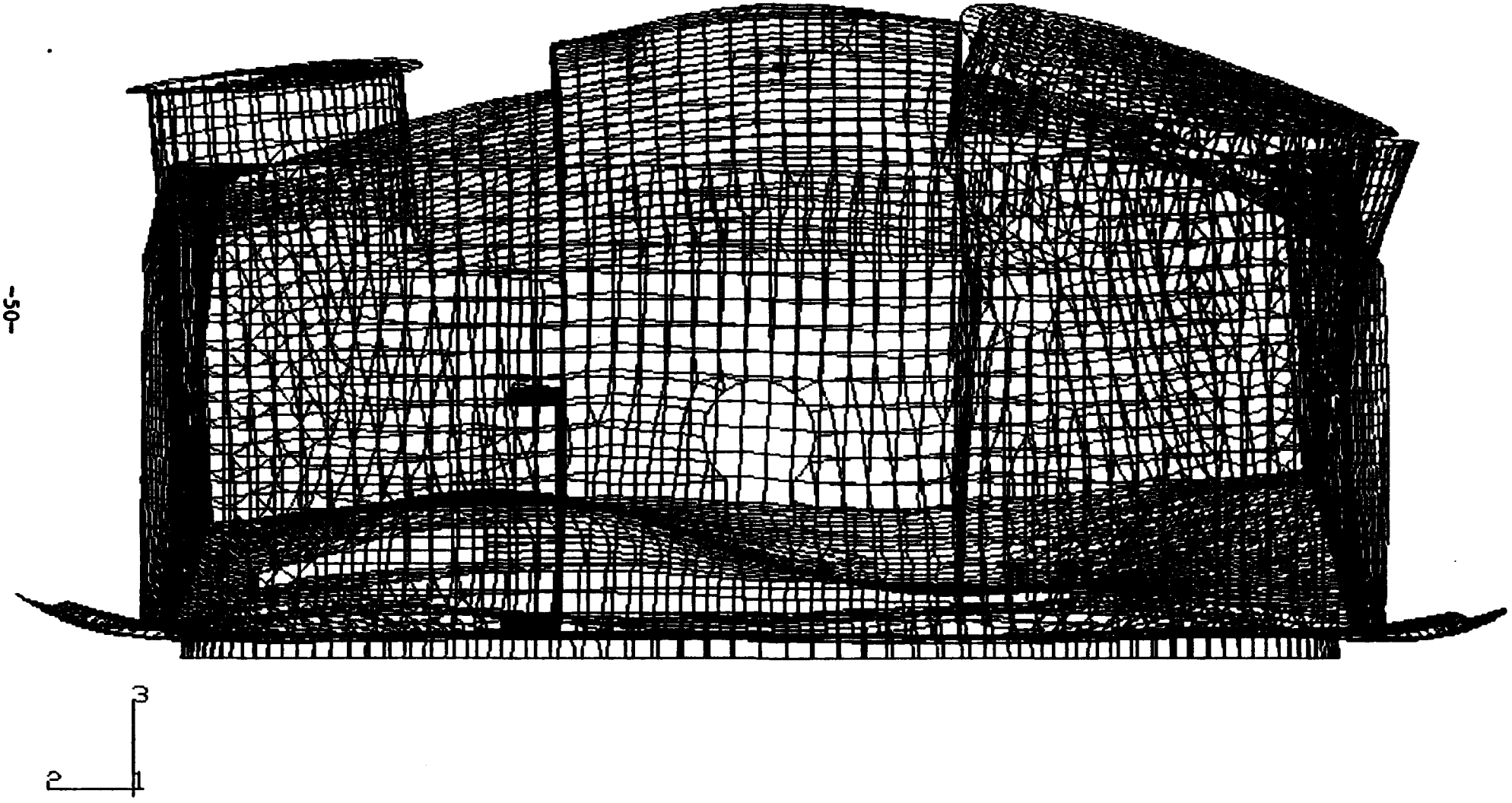

MAG. FACTOR =+1.2E+01

FIG. 6-26 DEFORMED SHAPE FOR MODE NO. 13 (FREQUENCY = 116 HZ)

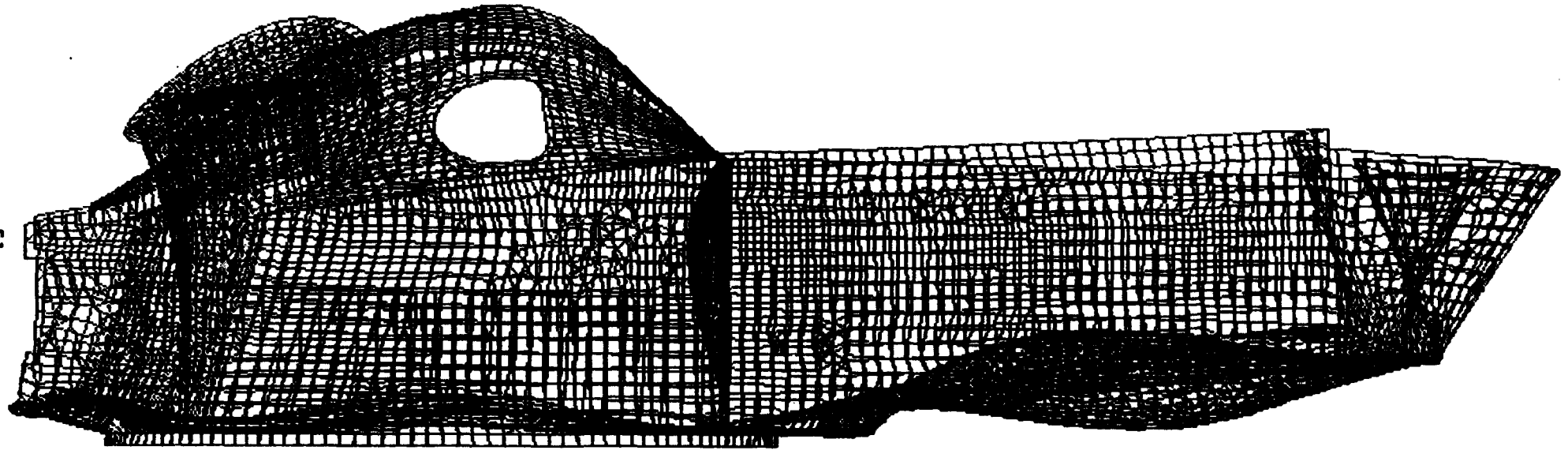

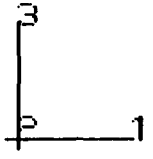

MAG. FACTOR =+2.0E+01

FIG.6-27 DEFORMED SHAPE FOR MODE NO. 13 (FREQUENCY = 116 HZ)

DISTRIBUTION LIST

	Copies
Commander Defense Technical Information Center Bldg 5, Cameron Station ATTN: DDAC Alexandria, VA 22304-9990	1
Manager Defense Logistics Studies Information Exchange ATTN: AMXMC-D Fort Lee, VA 23801-6044	1
Director U.S. Army Materiel Systems Analysis Activity ATTN: AMXSY-MP (Mr. Cohen) Aberdeen Proving Ground, MD 21005-5071	1
Commander U.S. Army Materiel Command ATTN: AMCRDA (Mr. R. O. Black) 5001 Eisenhower Ave Alexandria, VA 22333-0001	1
Commander U.S. Army Armament Research, Development and Engineering Center ATTN: SMCAR-CCB-DS,MR John Zweig Headquarters, Armament Munitions and Chemical Command Picatinny Arsenal, NJ 07806-5000	5
Commander U.S. Missile Command ATTN: AMSMI-IRD (Technical Director) Redstone Arsenal, AL 35898-5000	1
Commander U.S. Army Tank-Automotive Command ATTN: AMSTA-CF (Dr. K. J. Oscar) Warren, MI 48397-5000	1
Commander U.S. Army Tank-Automotive Command ATTN:Director of Eng. Design and Manufg Tech (AMSTA-TD),Mr Art.Adlam. Warren, MI 48397-5000	1

		COPIES
Commander U.S. Army Belvoir Research, Development and Engineering Center ATTN: STRBE-ZT Fort Belvoir, VA 22060-5606		1
Director Ballistic Research Laboratory ATTN: Technical Director Aberdeen Proving Ground, MD 21005-65066		1
Commander and Director Corps of Engineers Waterways Experimental Station ATTN: Technical Director P.O. Box 631 Vicksburg, MS 39181-0631		1
Project Office, CATTB Mr, Paul Cag	AMSTA-ZTT	3
Project Office, Block III	AMCPM-Block III	1
Project Manager, Abram Tank System	AMCPM,AMBS	1
Project Manager, Advanced Field Artillery System	AMCPM-AFAS	1
Project Manager, Future Infantry Fighting Vehicle	AMCMP-FIFV	1
Office of Heavy Equipment Transporter	SFAE-CS-TVH	1
System Engineering Directorate ATTN: Mr. Bill Madro	AMSTA-U	1
Mobility Technical Center DIrector: Mr. McClaland. AMSTA-R		1